In Japan, DAV-feron is commonly given to treat melanomas and shows minor adverse effects, including grade 1 hematotoxic effects.[6] Although treatment with interferon alfa-2b appears beneficial,[7] we used DAV-feron because the risk for teratogenicity and abortion appears low during the second and third trimester.

O'Meara et al[2] reported no difference in the distribution of stage, tumor thickness, or number of positive lymph nodes between pregnant women with melanomas and those without malignant neoplasms. Case reports are necessary to evaluate whether the disease-free interval and the survival rate differ in pregnancy-associated stage III melanomas from the overall 5-year survival rate, which is approximately 50% for stage III melanoma. Furthermore, it is important to report the efficacy of chemotherapy during pregnancy by monitoring the exact time of exposure, the dose given, and the frequency of treatment.

Isao Ishida, MD, PhD
Yuji Yamaguchi, MD, PhD
Atsushi Tanemura, MD, PhD
Ko Hosokawa, MD, PhD
Satoshi Itami, MD, PhD
Akimichi Morita, MD, PhD
Ichiro Katayama, MD, PhD

Correspondence: Dr Yamaguchi, Department of Geriatric and Environmental Dermatology, Nagoya City University Graduate School of Medical Sciences, 1-Kawasumi, Mizuho-cho, Mizuho-ku, Nagoya, 467-8601, Japan (yujin@med.nagoya-cu.ac.jp).

Financial Disclosure: None reported.

Funding/Support: This work was supported in part by the 1st Rohto Award, a grant from the 32nd Aichi Cancer Research Foundation, and grant-in-aid 18689028 from the Ministry of Education, Culture, Sports, Science and Technology of Japan (Dr Yamaguchi).

Additional Information: Drs Ishida and Yamaguchi contributed equally to this work, which was originally done at Osaka University Graduate School of Medicine, Osaka, Japan.

Additional Contributions: Toshiaki Nakamura, MD; Eriko Mabuchi, MD; Mirei Ri, MD; Yoko Nishida, MD; Ryuji Tsuji, MD; Noriko Umegaki, MD; Chika Ohata, MD; Mamori Tani, MD; Ryoko Minekawa, MD; and Tadashi Kimura, MD, critically reviewed this work.

1. Alexander A, Samlowski WE, Grossman D, et al. Metastatic melanoma in pregnancy: risk of transplacental metastases in the infant. *J Clin Oncol.* 2003;21(11):2179-2186.
2. O'Meara AT, Cress R, Xing G, Danielsen B, Smith LH. Malignant melanoma in pregnancy: a population-based evaluation. *Cancer.* 2005;103(6):1217-1226.
3. Li RH, Tam WH, Ng PC, Mok TS, Tam B, Lau TK. Microphthalmos associated with Dartmouth combination chemotherapy in pregnancy: a case report. *J Reprod Med.* 2007;52(6):575-576.
4. Dipaola RS, Goodin S, Ratzell M, Florczyk M, Karp G, Ravikumar TS. Chemotherapy for metastatic melanoma during pregnancy. *Gynecol Oncol.* 1997;66(3):526-530.
5. Harkin KP, Drumm JE, O'Brien P, Daly A. Metastatic malignant melanoma in pregnancy. *Ir Med J.* 1990;83(3):116-117.
6. Ueda E, Kishimoto S, Yasuno H. Statistical survey from 1982 to 1991 of 49 patients with malignant melanocytic tumors. *J Dermatol.* 1995;22(7):467-474.
7. Eggermont AM, Suciu S, MacKie R, et al; EORTC Melanoma Group. Post-surgery adjuvant therapy with intermediate doses of interferon alfa 2b versus observation in patients with stage IIb/III melanoma (EORTC 18952): randomised controlled trial. *Lancet.* 2005;366(9492):1189-1196.

Tunga penetrans: Description of a New Dermoscopic Sign—The Radial Crown

We agree with Bauer et al[1] and Di Stefani et al[2] regarding the dermoscopic features of *Tunga penetrans* described in earlier issues of the *Archives*, and we would like to describe here an additional dermoscopic finding for this disease. Tungiasis is an ectoparasitic skin disease caused by the female sand flea *T penetrans*. It is endemic to South and Central America, sub-Saharan Africa, the Caribbean, and Asia, where it represents a public health problem. The transmission of the flea occurs by walking barefoot in sands contaminated by feces of pigs and cows. The diagnosis is clinical, but dermoscopy is helpful and shows many characteristic features.[1,2]

We report here the case of a 70-year-old woman from Peru without notable medical history who developed a pruritic papule on the inside of the right foot. Our suspicion of tungiasis was confirmed by dermoscopic examination (**Figure 1**). As described by Bauer et al[1] and Di Stefani et al,[2] we found a black area with a plugged opening in the middle corresponding to the opening of the exoskeleton, a peripheral pigmented ring corresponding to the posterior abdomen of the flea, and many gray-blue blotches corresponding to the developing eggs in the abdomen of the flea.[3,4] We observed in our patient an additional novel dermoscopic feature, which we have termed the *radial crown*. Findings of histopathologic examination (**Figure 2**) showed this radial crown to be a zone of columnar hemorrhagic parakeratosis in a radial arrangement. This parakeratosis is analogous to that found in scabies infestation, possibly induced by the helper T-cell subtype 2 inflammatory reaction caused by the penetration of the flea into the skin of the human host.[5] We propose therefore to add the radial crown to the other typical dermoscopic features of tungiasis.

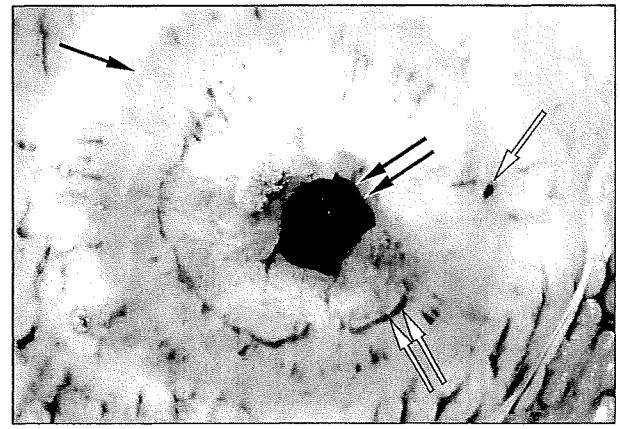

Figure 1. Dermoscopic features of tungiasis: a peripheral pigmented ring (single black arrow), a central dark area (double black arrows) and a brownish-gray blotch (single white arrow). The new dermoscopic finding is the "radial crown" (double white arrows).

0031-3998/09/6504-0453
PEDIATRIC RESEARCH

Vol. 65, No. 4, 2009
Printed in U.S.A.

Two Novel Mutations in the *ED1* Gene in Japanese Families With X-Linked Hypohidrotic Ectodermal Dysplasia

GUNADI, KENJI MIURA, MIKA OHTA, AKI SUGANO, MYEONG JIN LEE, YUMI SATO, AKIKO MATSUNAGA, KAZUHIRO HAYASHI, TATSUYA HORIKAWA, KAZUNORI MIKI, MARI WATAYA-KANEDA, ICHIRO KATAYAMA, CHIKAKO NISHIGORI, MASAFUMI MATSUO, YUTAKA TAKAOKA, AND HISAHIDE NISHIO

Department of Genetic Epidemiology [G., K.M., M.J.L., H.N.], Laboratory for Applied Genome Science and Bioinformatics [K.M., M.O., A.S., Y.T.], Department of Pediatrics [Y.S., M.M., H.N.], Department of Dermatology [A.M., K.H., T.H., C.H.], Kobe University Graduate School of Medicine, Kobe 650-0017, Japan; Department of Pediatrics [K.M.], Itami Municipal Hospital, Itami 664-8540, Japan; Department of Dermatology [M.W.-K., I.K.], Osaka University Graduate School of Medicine, Suita 565-0871, Japan

ABSTRACT: X-linked hypohidrotic ectodermal dysplasia (XLHED), which is characterized by hypodontia, hypotrichosis, and hypohidrosis, is caused by mutations in *EDI*, the gene encoding ectodysplasin-A (EDA). This protein belongs to the tumor necrosis factor ligand superfamily. We analyzed *EDI* in two Japanese patients with XLHED. In patient 1, we identified a 4-nucleotide insertion, c.119-120insTGTG, in exon 1, which led to a frameshift mutation starting from that point (p.L40fsX100). The patient's mother was heterozygous for this mutation. In patient 2, we identified a novel missense mutation, c.1141G>C, in exon 9, which led to a substitution of glycine with arginine in the TNFL domain of EDA (p.G381R). This patient's mother and siblings showed neither symptoms nor *EDI* mutations, so this mutation was believed to be a *de novo* mutation in maternal germline cells. According to molecular simulation analysis of protein structure and electrostatic surface, p.G381R increases the distance between K375 in monomer A and K327 in monomer B, which suggests an alteration of overall structure of EDA. Thus, we identified two novel mutations, p.L40fsX100 and p.G381R, in *EDI* of two XLHED patients. Simulation analysis suggested that the p.G381R mutation hampers binding of EDA to its receptor *via* alteration of overall EDA structure. **(*Pediatr Res* 65: 453–457, 2009)**

Hypohidrotic ectodermal dysplasia (HED) is a congenital disorder characterized by the impaired development of teeth (hypodontia), hair (hypotrichosis), and eccrine sweat glands (hypohidrosis) (1). Most HED patients have shown an X-linked inheritance pattern, although a minority of patients had an autosomal dominant or recessive trait (2,3).

The *EDI* gene responsible for XLHED was mapped to chromosome Xq12-q13 and was identified by positional cloning (4). *EDI* encodes the protein ectodysplasin-A (EDA) that belongs to the tumor necrosis factor ligand (TNFL) superfamily (5,6). EDA consists of a small N-terminal intracellular domain, a transmembrane domain, and a larger C-terminal extracellular domain containing a furin-cleavage site, a collagen-like domain, and a TNFL domain. The collagen-like domain has been believed to be necessary for trimerization of EDA proteins (7). However, it is not known whether the collagen-like domain is solely responsible for the trimerization: constructs of EDA-A1 and EDA-A2 lacking the collagen-like region can pack in the crystals as dimers of trimers (8). The TNFL domain has the ability to interact with the EDA receptor (EDAR) and X-linked ectodysplasin-A2 receptor (XEDAR) (9).

EDA-A1 and EDA-A2 are the longest EDA isoforms, but they differ by only an insertion/deletion of two amino acids (E308, V309) as determined by alternative splicing of *EDI* pre-mRNA. This insertion/deletion functions to regulate receptor-binding specificity, such that EDA-A1 binds EDAR, whereas EDA-A2 binds XEDAR (10). EDAR interacts with its adapter EDAR-associated death domain (EDARADD) to build an intracellular complex and activate the nuclear factor-κB pathway, which is essential for the proper development of ectodermal derivatives (3,11,12). *EDAR* and *EDARADD* are the genes responsible for the autosomal forms of HED (2,3,13).

Crystal structure analysis has provided a new understanding of EDA-A1 and EDA-A2. For example, higher-order assembly of the EDA trimers has been clarified. The crystallographic asymmetric unit of both EDA-A1 and EDA-A2 crystals contains more than one copy of the biologically relevant trimer. The EDA-A1 asymmetric unit comprises four trimers, and the EDA-A2 asymmetric unit comprises two trimers. Ligation of trimers into higher-order assemblies may increase receptor affinity by avidity or may change the geometry of the ligand-receptor complex (8).

Many mutations in *EDI* in various countries have been reported (14–17). In Japan, several mutations have been identified in XLHED patients (18–20). Affected males showed most or all of the typical phenotypes of XLHED. However, only a few studies have reported the relationship between nucleotide substitution and protein structure (8,21,22).

In this study, we analyzed the *EDI* gene in two unrelated Japanese patients with XLHED, and we identified two novel

Received September 5, 2008; accepted November 4, 2008.
Correspondence: Hisahide Nishio, M.D., Ph.D., Department of Genetic Epidemiology, Kobe University Graduate School of Medicine, 7-5-1 Kusunoki-cho, Chuo-ku, Kobe 650-0017, Japan; e-mail: nishio@med.kobe-u.ac.jp
Supported by a Grant-Aid from the Ministry of Education, Science, Sports and Culture of Japan.

Abbreviations: DHPLC, denaturing high-performance liquid chromatography; **EDA,** ectodysplasin-A; **HED,** hypohidrotic ectodermal dysplasia; **TNFL,** tumor necrosis factor ligand; **XLHED,** X-linked HED

mutations: p.L40fsX100 and p.G381R. The former was inherited from the mother, and the latter was a *de novo* mutation occurred in maternal germline cells. Our molecular simulation analysis of EDA suggested that the p.G381R mutation hampers the binding of EDA to its receptor *via* alteration of the overall structure of EDA.

PATIENTS AND METHODS

Patients. Two Japanese patients with XLHED were enrolled in this study. Informed consent was obtained from the parents before DNA sampling. This study was approved by the Kobe University ethical committee. One hundred healthy Japanese adults volunteered to participate in the study as control subjects.

Patient 1 was a 1-y-5-mo-old boy of unrelated parents in family A (Fig. 2*A*). He had no siblings. The mother was healthy from her appearance; she had no abnormal features and no missing permanent teeth. The patient was initially diagnosed with HED on the basis of his sparse, thin hair; lack of eyebrows and eyelashes; and characteristic facial appearance, including a prominent forehead and saddle nose. The qualitative sweating test with starch and iodine produced almost no response in the patient. The mother showed a slight decrease in sweat response, but she did not undergo further quantitative analysis. Histologic examination of the skin biopsy specimen showed complete lack of hair follicles, eccrine sweat glands, and sebaceous glands, which corresponded to the characteristic findings of HED (Fig. 1A). XLHED was diagnosed on the basis of molecular analysis of *ED1*.

Patient 2 was an 8-mo-old twin boy of unrelated parents in family B (Fig. 3*A*). His elder sister, twin brother, and parents were healthy and showed no dysmorphologic features. He was referred to a city hospital because of recurrent episodes of high temperature. The diagnosis of HED was based on his thin skin, sparse hair; lack of eyebrows; no teeth; and characteristic facial features, including a full forehead and saddle nose. The acetylcholine test demonstrated no sweat response in the patient. Histologic examination of the skin biopsy specimen revealed complete lack of hair follicles, eccrine sweat glands, and sebaceous glands (Fig. 1B). XLHED was diagnosed on the basis of molecular analysis of *ED1*.

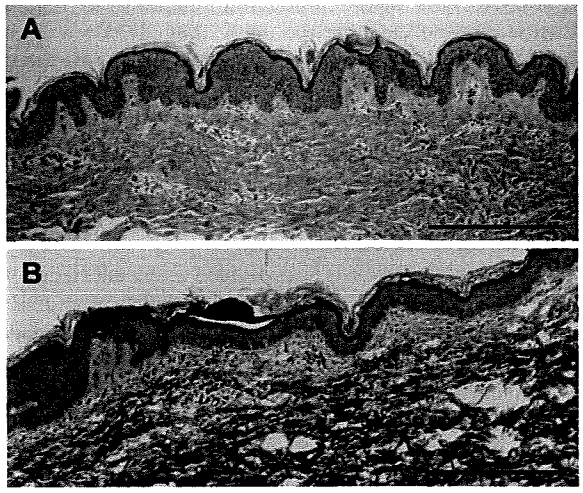

Figure 1. Histologic examination of the skin biopsy specimen. (*A*) Patient 1. H&E staining. Scale bar, 0.5 mm. (*B*) Patient 2. H&E staining. Scale bar, 0.5 mm. Both patients showed complete lack of hair follicles, eccrine sweat glands, and sebaceous glands.

DNA extraction. Genomic DNA was extracted from 2–5 mL of whole blood from each individual by using a DNA extraction kit (SepaGene; Sanko Junyaku, Tokyo, Japan), according to the manufacturer's instructions. The extracted DNA samples were stored at –20°C until analysis.

Polymerase chain reaction. PCR was carried out by using a PC 701 thermal cycler (Astec, Tokyo, Japan). Table 1 shows the primer sequences for *ED1* analysis.

Denaturing HPLC (DHPLC). To screen for a mutation in *ED1*, DHPLC analysis was performed according to our previous reports (23,24). Hybridization of the PCR product mixture of the test DNA with nucleotide substitution and reference DNA without nucleotide substitution produced a heteroduplex peak in the DHPLC chart. The appearance of this heteroduplex peak suggested the presence of a nucleotide substitution in the PCR-amplified fragment. The DHPLC conditions, including column temperatures (Table 1), were determined empirically to maximize resolution of the heteroduplex and homoduplex peaks.

DNA sequencing. To identify and confirm the mutation, direct sequencing analysis was performed with a BigDye Terminator V3.0 Cycle Sequencing Kit (Applied Biosystems, Foster City, CA) and a genetic analyzer (ABI Prism 310; Applied Biosystems), with DNA Sequencing Analysis Software (Applied Biosystems).

Skewed X-chromosome inactivation assay. To determine the X-chromosome inactivation status of the mother of family A, a manifested carrier of XLHED, we quantified the activated and inactivated CpG dinucleotides in exon 1 of the androgen receptor gene (*AR*) by the method described in our previous report (25). To explain briefly, unmethylated (activated) and methylated (inactivated) alleles were measured *via* a combination of DNA digestion by *Hpa*II and PCR amplification of digested and nondigested products. *Hpa*II digested unmethylated CpG but not methylated CpG. PCR amplified only nondigested products, *i.e.* the inactivated allele. The degree of inactivation skewing to one allele was calculated according to the formula presented by Lau *et al.* (26).

Parentage testing. To confirm that all siblings in family B were born to the same parents, parentage testing was performed. Fifteen additional loci on 13 chromosomes were genotyped in all family members by using AmpFLSTR PCR Amplification Kits (Applied Biosystems). The loci tested were D3S1358, vWA, D16S539, D2S1338, D8S1179, D21S11, D18S51, D19S433, THo1, FGA, D5S818, D13S317, D7S820, TPOX, and CSF1PO. Genomic DNA was amplified in a standard PCR reaction, and alleles were analyzed *via* the ABI PRISM 310 Genetic Analyzer with GeneScan and Genotyper software programs (Applied Biosystems).

Molecular simulation analysis of the protein structure and the electrostatic surface. The three-dimensional structures of EDA-A1 and EDA-A2 were derived from Protein Data Bank (accession numbers: EDA-A1, 1RJ7; EDA-A2, 1RJ8). The hydrogen atoms in these model structures were added by means of PyMOL software (27). Following preparation of p.G381R mutants of EDA-A1 and EDA-A2 by means of SWISS-MODEL and Swiss-PDB Viewer (28), the mutant coordinates were optimized by using the MINIMIZE program of the TINKER software package (29) with the AMBER99 force field parameter. The minimizations were executed for root mean square (RMS) gradient values of 0.01 kcal/mol/Å. Then, the molecular structure and electrostatic surface were analyzed by using PyMOL software with the APBS (Adaptive Poisson-Boltzmann Solver) plugin (30).

Table 1. *Primer sets used for amplification of the* ED1 *gene and DHPLC temperature*

Primers name	Forward (5′->3′)	Reverse (5′->3′)	Fragment size (bp)	Annealing temp. (°C)	DHPLC temp (°C)
ED1–1A	TGAACGGCTGAGGCAGACG	TCCGAGCGCAACTCTAGGTA	262	66	62.8
ED1–1B	GCCTGCTCTTCCTGGGTTT	GCCCCTACTAGGTGACTCA	298	58	62.1
ED1–3	TGTTGGCTATGACTGAGTGG	GCCCTACCAAGAAGGTAGTT	248	56	54.0
ED1–4	CTGTGAGACTCCCTCAAATT	ATAACAGACAGACAATGCTGA	257	60	56.4
ED1–5	TGGGCAACAGAGCAGGACT	ACCCACTCCTGCTCTCCTA	306	70	60.4
ED1–6	GAATAAAGCTCAGACAGGGC	AATCTCCGGGGTGTTCTCAT	273	62	58.1
ED1–7	AGGATGGAAACATGGGACTG	AGGGCATGATGGAGCAAAGA	276	62	58.3
ED1–8	CTGTTGCCTCGATTATTCTG	TGCACCGGATCTGCATTCT	242	56	56.9
ED1–9	CACCCTCTCTTTCCTCTCTT	TTAGAGGTTCTGGGAGTCCT	373	60	61.6

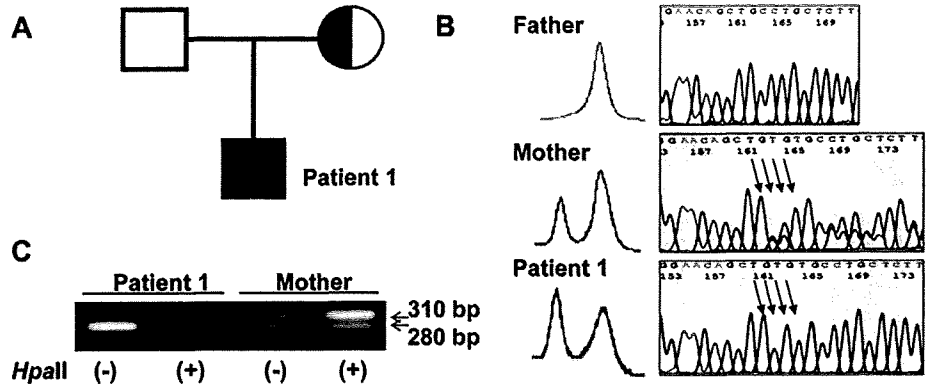

Figure 2. Family A with XLHED. (*A*) Pedigree. (*B*) DHPLC screening and direct DNA sequencing of *EDI* exon 1. The patient carried a c.119-120insTGTG in *EDI* exon 1, which made a premature stop codon at amino acid 100 (p.L40fsX100). His mother was heterozygous for the mutation. Arrows indicate the TGTG insertion. (*C*) X-chromosome inactivation assay. The 310-bp band was from the normal allele, and the 280-bp band was from the affected allele. In patient 1, no amplification of the 280-bp band was obtained, because the patient X-chromosome is not methylated. In his mother, with *Hpa*II treatment produced a higher intensity 310-bp band compared with the 280-bp band, which suggests that the normal allele was mainly inactivated by methylation. The degree of skewed X-chromosome inactivation toward the normal allele was calculated as 80%.

RESULTS

Patient 1 and Family A

Identification of a novel insertion mutation. A heteroduplex peak in the DHPLC chart for *EDI* exon 1 suggested the presence of a mutation in the patient and his mother (Fig. 2*B*). Direct sequencing showed that the patient had a 4-bp insertion between nucleotides 119 and 120 of *EDI* exon 1 (c.119-120insTGTG) (Fig. 2*B*). The mother was heterozygous for the mutation. The insertion c.119-120insTGTG led to a frameshift mutation starting from that point and would result in truncation of the protein at amino acid 100 (p.L40fsX100).

Determination of skewed X-chromosome inactivation. Figure 2*C* shows the result of the skewed X-chromosome inactivation assay. The affected allele of patient 1 was digested completely by *Hpa*II treatment, and no amplification of the 280-bp band of the affected allele was observed. For his mother, two bands, the 310-bp band from the normal allele and the 280-bp band from the affected allele, were obtained with and without *Hpa*II treatment. Without *Hpa*II treatment, the 310-bp and 280-bp bands manifested the same intensity. However, with *Hpa*II treatment, the 310-bp band had a much higher intensity compared with the 280-bp band, which suggests that the normal allele was mainly inactivated by methylation. The degree of skewed X-chromosome inactivation toward the normal allele was calculated to be 80%, *i.e.* only 20% of the activated X-chromosome was normal.

Patient 2 and Family B

Identification of a novel missense mutation. A heteroduplex peak in the DHPLC chart for *EDI* exon 9 suggested the presence of a mutation in the patient (Fig. 3*B*). Direct DNA sequencing showed that the patient had a G-to-C transversion at nucleotide 1141 (Fig. 3*C*). This c.1141G>C transversion led to substitution of glycine with arginine at amino acid 381 (p.G381R) in the TNFL domain. p.G381R likely affects the binding of EDA to its receptor; the glycine residue at amino

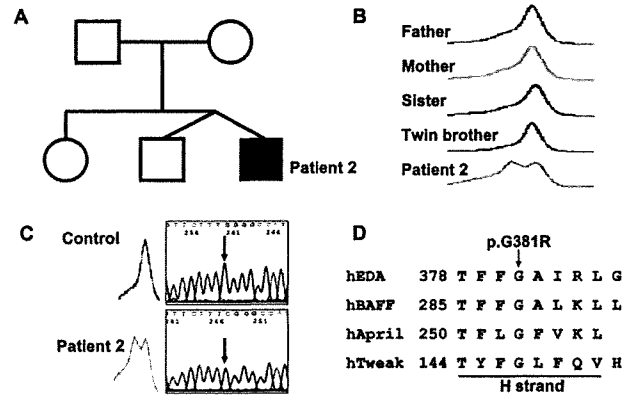

Figure 3. Family B with XLHED. (*A*) Pedigree. (*B*) DHPLC screening of *EDI* exon 9. DHPLC demonstrated a heteroduplex peak for patient 2 but not other family members. (*C*) Direct DNA sequencing of *EDI* exon 9. The patient carried a c.1141G>C in *EDI* exon 9, which led to substitution of glycine with arginine at amino acid 381 (p.G381R). The arrow indicates the c.1141G>C. (*D*) Amino acid sequence alignments of EDA and its closest relatives in the H-strand of the TNFL domain. Bold letters mean conserved amino acids. The glycine at amino acid 381 in EDA is highly conserved among the TNFL superfamily.

acid 381 is highly conserved among TNFL domains in TNFL superfamily members (Fig. 3*D*).

DHPLC did not detect the index transversion in family members. The transversion in the patient may be a maternal germline mutation, because parentage testing verified the relationships among family members with a cumulative likelihood ratio of more than 99.99% (data not shown).

To test the possibility that c.1141G>C in *EDI* was a polymorphism, we screened 100 Japanese control subjects for the transversion. None carried this transversion, which suggests that it is not a polymorphism but is instead a disease-causing mutation.

Molecular structure and electrostatic surface of G381R mutants. To investigate whether p.G381R could alter the

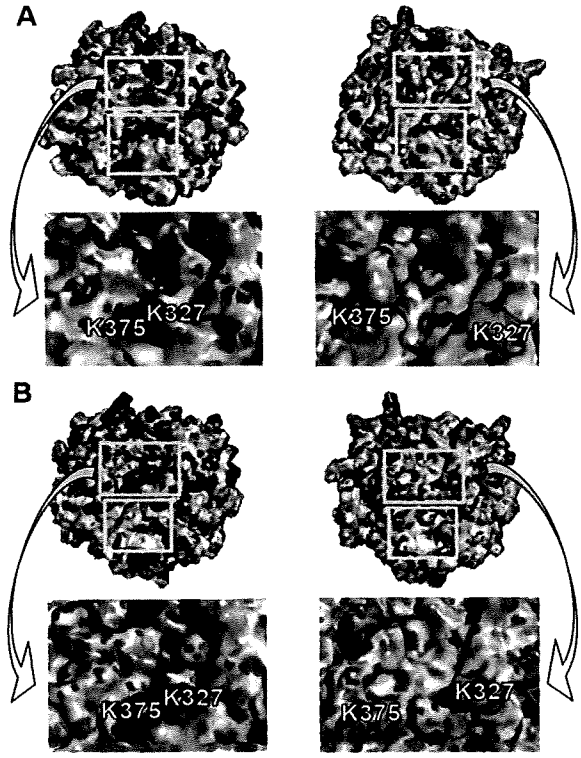

Figure 4. Effect of the p.G381R mutation on the electrostatic surface of EDA-A1 and EDA-A2. (*A*) Electrostatic surfaces of wild-type EDA-A1 (*left*) and p.G381R-mutant EDA-A1 (*right*), with predicted receptor binding sites (*yellow boxes*). As shown in the enlargements of the upper yellow boxed areas, the p.G381R mutation increased the distance between K375 in monomer A and K327 in monomer B. (*B*) Electrostatic surfaces of wild-type EDA-A2 (*left*) and p.G381R-mutant EDA-A2 (*right*), with predicted receptor binding sites (*yellow boxes*). As shown in the enlargements of the upper boxed areas, similar to EDA-A1, the p.G381R mutation increased the distance between K375 in monomer A and K327 in monomer B.

overall structure of EDA, the electrostatic surface and the molecular structure were analyzed by using wild type and simulated mutant molecules. Figure 4*A* and *B* show the molecular surfaces of wild-type and p.G381R-mutated EDA colored according to the calculated electrostatic surface potential. Blue indicates positive (maximum +10 kT/e), white indicates neutral, and red indicates negative (minimum −10 kT/e). The EDA surface contains the putative receptor-binding site along the monomer–monomer interface. The relatively large receptor interaction areas (upper and lower yellow boxes in Fig. 4*A* and *B*) include dispersed binding determinant parts. The mutation alters the positively charged area in the receptor binding sites (upper yellow boxes in Fig. 4*A* and *B*) of EDA. In wild-type isoforms, K375 in monomer A and K327 in monomer B are adjacent, whereas in p.G381R-mutant isoforms, the two amino acids are separated by a considerable distance.

DISCUSSION

Mutations. We identified two novel mutations in *EDI* in two Japanese patients with XLHED. Patient 1 carried a new 4-bp insertion, c.119-120insTGTG, which led to a frameshift mutation starting from amino acid 40 and made a stop codon at amino acid 100 in EDA (p.L40fsX100). The truncated EDA would lack part of the collagen-like domain and the whole TNFL domain. The collagen-like domain is crucial for trimerization of EDA, and the TNFL domain is required for binding of EDA to its receptor (7). However, it is not known whether the collagen-like domain is solely responsible for the trimerization, as described in the Introduction section. Schneider *et al.* (9) also reported that in-frame deletions in collagen-like domain do not affect the ability of EDA to trimerize nor to further multimerize, suggesting that the collagen-like domain may serve additional functions. Thus, the 4-bp insertion may disrupt the functions of the EDA protein because of the loss two important functional domains. Patient 2 carried a novel missense mutation, c.1141G>C, which led to the substitution of glycine with arginine at amino acid 381 in EDA (p.G381R). The mutation is located in the TNFL domain of the EDA protein. Several mutations in the TNFL domain have previously been reported (8,9,22). Schneider *et al.* (9) showed that all missense mutations in the TNFL domain resulted in abolished or impaired binding of EDA to its receptors.

Inheritance traits. The mother of patient 1 had no symptoms except for slightly decreased sweating, with X-chromosome inactivation being skewed mainly toward the normal allele in blood cells. Carriers who are heterozygous for an XLHED mutation may have variable clinical features (14,17,31,32). Lexner *et al.* (17) reported that in two female carriers with pronounced clinical symptoms, the normal allele in their blood cells was mainly inactivated. Martínez *et al.* (31) suggested that skewed X-chromosome inactivation in blood cells can explain symptomatic differences among female carriers. However, the finding for our family A were not consistent with such reports. Our result suggests that X-chromosome inactivation is different in skin from blood cells: ectodermal and mesodermal tissues may differ with regard to factors related to X-chromosome inactivation. It also leads us to the idea that unlike the inference in previous reports, skewed X-chromosome inactivation in blood cells does not predict the clinical situation in the carrier status of XLHED.

The p.G381R mutation in patient 2 was a germline mutation. The recurrence risk of the germline mutation may depend on the proportions of germ cells with and without the mutation (24). The possibility of mutation recurrence in the next male sibling of a patient should be explained to parents during genetic counseling, even though the disease-causing mutation was identified as a *de novo* mutation and the risk of recurrence of the disease cannot be exactly determined.

Protein structure. The p.G381R mutation in patient 2 replaced the small amino acid, glycine, with a larger one, arginine, that could not be accommodated structurally. Hymowitz *et al.* (8) divided the disease-causing mutations that affect the TNFL domain of EDA into three groups: 1) mutations that probably affect the overall structure of EDA, 2) mutations that affect the receptor binding site, and 3) mutations whose effect is uncertain but that may define a novel interaction site. It is most reasonable to expect that p.G381R belongs to the first group and may affect EDA function *via* alteration of overall EDA structure. Our simulation data offered some evidence for this hypothesis. The mutation in-

creased the distance between K375 in monomer A and K327 in monomer B, which resulted in a drastic change in the electrostatic surface and surface conformation of the receptor binding site (upper boxes in Fig. 4*A* and *B*).

The question then arises: how does this p.G381R-induced alteration in structure affect EDA function? One possible explanation is that the electrostatic and structural changes in the surface caused by the mutation may hamper receptor binding. It should be noted that the mutation produced a large alteration in the "upper box" part of the receptor-binding site and a small alteration in the "lower box" part. This finding suggests that these parts of the receptor-binding site play different roles, that is, maintaining binding affinity and providing the receptor specificity, respectively. Another possible explanation is that unexpected physiochemical changes related to p.G381R may have a negative effect on receptor binding or assembly of the three monomers. An additional possibility is that the mutation alters the solubility or folding properties of EDA, which are related to its secretion by cells.

In conclusion, we found two novel mutations, one a frameshift (p.L40fsX100) and one a missense (p.G381R), in *ED1* and discussed their inheritance trait in two unrelated families with XLHED. Molecular simulation analysis of the structure of the EDA protein suggested that the missense mutation hampers the binding of EDA into its receptor *via* alteration of the overall structure of EDA.

Acknowledgments. We thank Dr. Ahmad Hamim Sadewa and Dr. Teguh Haryo Sasongko (Kobe University Graduate School of Medicine) for their technical assistance and Drs. Surini Yusoff and Indra Sari Kusuma Harahap (Kobe University Graduate School of Medicine) for their helpful comments on interpretation of the data.

REFERENCES

1. McKusick VA 1998 Mendelian Inheritance in Man, 12th Ed. Johns Hopkins University Press, Baltimore, pp 3307–3309
2. Monreal AW, Ferguson BM, Headon DJ, Street SL, Overbeek PA, Zonana J 1999 Mutations in the human homologue of mouse *dl* cause autosomal recessive and dominant hypohidrotic ectodermal dysplasia. Nat Genet 22:366–369
3. Headon DJ, Emmal SA, Ferguson BM, Tucker AS, Justice MJ, Sharpe PT, Zonana J, Overbeek PA 2001 Gene defect in ectodermal dysplasia implicates a death domain adapter in development. Nature 414:913–916
4. Kere J, Srivastava AK, Montonen O, Zonana J, Thomas N, Ferguson B, Munoz F, Morgan D, Clarke A, Baybayan P, Chen EY, Ezer S, Saarialho-Kere U, de la Chapelle A, Schlessinger D 1996 X-linked anhidrotic (hypohidrotic) ectodermal dysplasia is caused by mutation in a novel transmembrane protein. Nat Genet 13:409–416
5. Bayés M, Hartung AJ, Ezer S, Pispa J, Thesleff I, Srivastava AK, Kere J 1998 The anhidrotic ectodermal dysplasia gene (EDA) undergoes alternative splicing and encodes ectodysplasin-A with deletion mutations in collagenous repeats. Hum Mol Genet 7:1661–1669
6. Monreal AW, Zonana J, Ferguson B 1998 Identification of a new splice form of the EDA1 gene permits detection of nearly all X-linked hypohidrotic ectodermal dysplasia mutations. Am J Hum Genet 63:380–389
7. Ezer S, Bayés M, Elomaa O, Schlessinger D, Kere J 1999 Ectodysplasin is a collagenous trimeric type II membrane protein with a tumor necrosis factor-like domain and co-localizes with cytoskeletal structures at lateral and apical surfaces of cells. Hum Mol Genet 8:2079–2086
8. Hymowitz SG, Compaan DM, Yan M, Wallweber HJ, Dixit VM, Starovasnik MA, de Vos AM 2003 The crystal structures of EDA-A1 and EDA-A2: splice variants with distinct receptor specificity. Structure 11:1513–1520
9. Schneider P, Street SL, Gaide O, Hertig S, Tardivel A, Tschopp J, Runkel L, Alevizopoulos K, Ferguson BM, Zonana J 2001 Mutations leading to X-linked hypohidrotic ectodermal dysplasia affect three major functional domains in the tumor necrosis factor family member ectodysplasin-A. J Biol Chem 276:18819–18827
10. Yan M, Wang LC, Hymowitz SG, Schilbach S, Lee J, Goddard A, de Vos AM, Gao WQ, Dixit VM 2000 Two-amino acid molecular switch in an epithelial morphogen that regulates binding to two distinct receptors. Science 290:523–527
11. Yan M, Zhang Z, Brady JR, Schilbach S, Fairbrother WJ, Dixit VM 2002 Identification of a novel death domain-containing adaptor molecule for ectodysplasin-A receptor that is mutated in crinkled mice. Curr Biol 12:409–413
12. Mikkola ML, Thesleff I 2003 Ectodysplasin signaling in development. Cytokine Growth Factor Rev 14:211–224
13. Bal E, Baala L, Cluzeau C, El Kerch F, Ouldim K, Hadj-Rabia S, Bodemer C, Munnich A, Courtois G, Sefiani A, Smahi A 2007 Autosomal dominant anhidrotic ectodermal dysplasias at the EDARADD locus. Hum Mutat 28:703–709
14. Vincent MC, Biancalana V, Ginisty D, Mandel JL, Calvas P 2001 Mutational spectrum of the ED1 gene in X-linked hypohidrotic ectodermal dysplasia. Eur J Hum Genet 9:355–363
15. Visinoni AF, de Souza RL, Freire-Maia N, Gollop TR, Chautard-Freire-Maia EA 2003 X-linked hypohidrotic ectodermal dysplasia mutations in Brazilian families. Am J Med Genet A 122:51–55
16. Zhao J, Hua R, Zhao X, Meng Y, Ao Y, Liu Q, Shang D, Sun M, Lo WH, Zhang X 2008 Three novel mutations of the EDA gene in Chinese patients with X-linked hypohidrotic ectodermal dysplasia. Br J Dermatol 158:614–617
17. Lexner MO, Bardow A, Juncker I, Jensen LG, Almer L, Kreiborg S, Hertz JM 2008 X-linked hypohidrotic ectodermal dysplasia. Genetic and dental findings in 67 Danish patients from 19 families. Clin Genet 74:252–259
18. Yotsumoto S, Fukumaru S, Matsushita S, Oku T, Kobayashi K, Saheki T, Kanzaki T 1998 A novel point mutation of the EDA gene in a Japanese family with anhidrotic ectodermal dysplasia. J Invest Dermatol 111:1246–1247
19. Aoki N, Ito K, Tachibana T, Ito M 2000 A novel arginine → serine mutation in EDA1 in a Japanese family with X-linked anhidrotic ectodermal dysplasia. J Invest Dermatol 115:329–330
20. Hashiguchi T, Yotsumoto S, Kanzaki T 2003 Mutations in the ED1 gene in Japanese families with X-linked hypohidrotic ectodermal dysplasia. Exp Dermatol 12:518–522
21. RamaDevi AR, Reddy EC, Ranjan S, Bashyam MD 2008 Molecular genetic analysis of patients from India with hypohidrotic ectodermal dysplasia reveals novel mutations in the EDA and EDAR genes. Br J Dermatol 158:163–167
22. Li S, Li J, Cheng J, Zhou B, Tong X, Dong X, Wang Z, Hu Q, Chen M, Hua ZC 2008 Non-syndromic tooth agenesis in two Chinese families associated with novel missense mutations in the TNF domain of EDA (ectodysplasin A). PLoS One 3:e2396
23. Sutomo R, Akutsu T, Takeshima Y, Nishio H, Sadewa AH, Harada Y, Matsuo M 2002 Rapid SMN1 deletion test using DHPLC to screen patients with spinal muscular atrophy. Am J Med Genet 113:225–226
24. Sadewa AH, Sasongko TH, Gunadi, Lee MJ, Daikoku K, Yamamoto A, Yamasaki T, Tanaka S, Matsuo M, Nishio H 2008 Germ-line mutation of KCNQ2, p.R213W, in a Japanese family with benign familial neonatal convulsion. Pediatr Int 50:167–171
25. Ishihara H, Kanda F, Nishio H, Sumino K, Chihara K 2001 Clinical features and skewed X-chromosome inactivation in female carriers of X-linked recessive spinal and bulbar muscular atrophy. J Neurol 248:856–860
26. Lau AW, Brown CJ, Peñaherrera M, Langlois S, Kalousek DK, Robinson WP 1997 Skewed X-chromosome inactivation is common in fetuses or newborns associated with confined placental mosaicism. Am J Hum Genet 61:1353–1361
27. DeLano WL 2002 The PyMOL Molecular Graphics System. Available at: http://www.pymol.org Accessed August 30, 2008
28. Guex N, Peitsch MC 1997 SWISS-MODEL and the Swiss-PdbViewer: an environment for comparative protein modeling. Electrophoresis 18:2714–2723
29. Ren P, Ponder JW 2003 Polarizable atomic multipole water model for molecular mechanics simulation. J Phys Chem B 107:5933–5947
30. Baker NA, Sept D, Joseph S, Holst MJ, McCammon JA 2001 Electrostatics of nanosystems: application to microtubules and the ribosome. Proc Natl Acad Sci USA 98:10037–10041
31. Martínez F, Millán JM, Orellana C, Prieto F 1999 X-linked anhidrotic (hypohidrotic) ectodermal dysplasia caused by a novel mutation in EDA1 gene: 406T>G (Leu55Arg). J Invest Dermatol 113:285–286
32. Vincent MC, Cossée M, Vabres P, Stewart F, Bonneau D, Calvas P 2002 Pitfalls in clinical diagnosis of female carriers of X-linked hypohidrotic ectodermal dysplasia. Arch Dermatol 138:1256–1258

Virchows Arch
DOI 10.1007/s00428-010-0880-1

ORIGINAL ARTICLE

Polymorphous lymphoproliferative disorder: a clinicopathological analysis

Naoto Nakamichi · Naoki Wada · Masaharu Kohara · Shirou Fukuhara · Haruo Sugiyama · Hiroyasu Ogawa · Masayuki Hino · Akihisa Kanamaru · Yuzuru Kanakura · Eiichi Morii · Katsuyuki Aozasa

Received: 7 October 2009 / Revised: 2 December 2009 / Accepted: 3 January 2010

Abstract Lymphoproliferative disorder (LPD) with polymorphous composition of proliferation (polymorphous LPD), containing large lymphoid cells together with small lymphocytes, plasma cells, macrophages, and/or eosinophils, is found in individuals with immunodeficiency conditions. Clinicopathological findings in 19 cases of polymorphous LPD registered with the Osaka Lymphoma Study Group, Osaka, Japan, were analyzed; they represented 0.4% of the registered cases. In six cases, there was a history of rheumatoid arthritis; five of them had received immunosuppressive agents. There were no acquired immunodeficiency syndrome cases or organ transplant recipients. Southern blotting and/or polymerase chain reaction (PCR)-based clonality analysis revealed monoclonal B cell and T cell proliferation in eight and six cases (B- and T-LPD), respectively, and polyclonality in one. In B-LPD, there was polymorphous proliferation, containing large B-lymphoid cells, while medium-to-large T lymphoid cells with occasional eosinophilic infiltration were seen in T-LPD. Epstein–Barr virus (EBV) was detected in three of eight B-LPD, four of six T-LPD, and one of one polyclonal LPD. The prognosis was not favorable; the 3-year overall survival rate was 49.7± 17.3%. Thus, polymorphous LPD is relatively rare in Japan and is a heterogeneous disease with monoclonal proliferation of B or T cells; additionally, it is occasionally EBV-associated, and behaves as an aggressive lymphoma.

Supported in part by a grant (20014012) from the Ministry of Education, Science, Culture, and Sports, Japan.

N. Nakamichi · N. Wada · M. Kohara · E. Morii · K. Aozasa (✉)
Department of Pathology (C3),
Osaka University Graduate School of Medicine,
2-2 Yamadaoka,
Suita, Osaka 565-0871, Japan
e-mail: aozasa@molpath.med.osaka-u.ac.jp

N. Nakamichi · S. Fukuhara
First Department of Internal Medicine,
Kansai Medical University,
Osaka, Japan

H. Sugiyama
Department of Functional Diagnostic Science,
Osaka University Graduate School of Medicine,
Osaka, Japan

H. Ogawa
Division of Hematology, Department of Internal Medicine,
Hyogo College of Medicine,
Nishinomiya, Hyogo, Japan

M. Hino
Department of Clinical Hematology and Clinical Diagnostics,
Graduate School of Medicine, Osaka City University,
Osaka, Japan

A. Kanamaru
Division of Hematology, Department of Internal Medicine,
Kinki University School of Medicine,
Osaka, Japan

Y. Kanakura
Department of Hematology and Oncology,
Osaka University Graduate School of Medicine,
Osaka, Japan

Published online: 29 January 2010

Keywords Lymphoproliferative disorder · Polymorphous · T cell · B cell · Clonality · EBV

Introduction

Polymorphous composition of proliferation containing large lymphoid cells together with small lymphocytes, plasma cells, macrophages, and/or eosinophils is a complex issue in diagnosis: the possible spectrum ranges from reactive changes, including infectious diseases, to neoplastic diseases, such as peripheral T cell lymphoma (PTCL), and Hodgkin lymphoma (HL). In PTCL, tumor cells secrete various cytokines that induce infiltration of inflammatory cells, resulting in polymorphous composition of proliferation. The neoplastic nature of PTCL can be judged based on the presence of medium-to-large T cells showing nuclear hyperchromasia and pleomorphism, with the appearance of bizarre cells, and can be confirmed by the presence of clonal T cells [1].

Polymorphous composition of proliferation devoid of neoplastic-looking T lymphoid cells is usually found in individuals with immunodeficiency conditions, including acquired immunodeficiency syndrome (AIDS) and transplant recipients receiving immunosuppressive drugs, and is referred to as polymorphous lymphoproliferative disorder (LPD) [2]. It is well known that polymorphous LPD can also develop in patients with rheumatoid arthritis (RA) receiving methotrexate (MTX; i.e., MTX-associated LPD, MTX-LPD) [1]. Among the newly listed categories in the updated World Health Organization (WHO) classification (2008), some cases of Epstein–Barr virus (EBV)-positive diffuse large B cell lymphoma (DLBCL) in the elderly, and also show a histological picture resembling polymorphous LPD [1]. EBV-positive DLBCL of the elderly (EBV + DLBCL-E) is defined as a lymphoma that occurs in patients >50 years with no known immunodeficiency.

Polymorphous LPD is occasionally encountered in routine clinical practice: some patients have a history of organ transplantation or RA treated with MTX, but others have no sign of immunological abnormality. These findings suggest that polymorphous LPD actually comprises a heterogeneous disease with differing etiologies. A previous immunophenotypic study suggested that the predominant proliferating cells were B cells in most polymorphous LPD cases, with T cells being much less frequent [2]. In the present study, we reviewed cases of polymorphous LPD registered with the Osaka Lymphoma Study Group (OLSG). Clinicopathological findings and the presence or absence of B or T cell clones, together with any association with EBV, were analyzed to clarify which diseases are included in "polymorphous LPD" encountered in routine practice in Japan.

Materials and methods

Patients

Between November 1999 and November 2008, in total, 4,422 cases of malignant lymphomas and related conditions were registered with the OLSG. Histological specimens, obtained by biopsy, were fixed in 10% formalin, and routinely processed for paraffin embedding. Histological sections cut at 4 μm were stained with hematoxylin and eosin, and immunoperoxidase procedures. All histological sections were reviewed by one author (KA). Of these 4,422 cases, 19 (0.4%) were diagnosed as polymorphous LPD after careful differential diagnosis from PTCL-not otherwise specified (NOS), HL, and reactive conditions, through evaluation of histological specimens, flow cytometry data, and molecular analyses. The polymorphous populations included neither diagnostic Reed-Sternberg (RS) cells nor a substantial number of medium-to-large T cells with nuclear hyperchromasia, and variable numbers of bizarre cells with multilobed nuclei, indicating that diagnoses of HL or PTCL were unlikely in these cases. Adequate clinical information was available for 18 patients.

The follow-up period for survivors ranged from 1 to 60 (median, 18) months. Information for therapeutic modalities was available in 17 cases: anthracycline-based chemotherapy in nine patients (53%), rituximab with or without combination chemotherapy, mostly cyclophosphamide, doxorubicin, vincristine, and prednisolone (CHOP), in six, and allogeneic bone marrow transplantation after four cycles of chemotherapy in one. One case with RA showed spontaneous partial remission of LPD after withdrawal of MTX, and another case died before the start of therapy.

Evaluation of clonality for B and T cells

DNA was extracted from paraffin-embedded samples in 17 cases, as described previously [3]. PCR-based assessment of rearrangement in the immunoglobulin, T-cell receptor (TCR), *BCL1-IGH*, and *BCL2-IGH* genes was performed using the BIOMED-2 PCR protocol, as described previously [4]. Amplified products were electrophoresed in 6% polyacrylamide gels. A PCR mixture with no DNA was used as a negative control, and a case of lymphoid hyperplasia or peripheral mononuclear cells as a polyclonal control. Clonality analyses were not performed in two cases because no paraffin-embedded samples were available.

Immunohistochemistry

An immunohistochemical study on the paraffin sections was conducted using the Envision+ system (DAKO, Carpinteria, CA, USA). Monoclonal antibodies used and

their dilutions were CD20 (1:400), CD3 (1:50), CD8 (1:100), CD30 (1:50; DakoCytomation, Glostrup, Denmark), and CD4 (1:40; NovoCastra, Newcastle, UK).

Classification of cases, according to the WHO scheme (2008)

Based on clinical, histological, immunohistochemical, and molecular data, the present cases were classified according to the WHO scheme (2008) [1]. Briefly, cases with monoclonal rearrangement of the TCR gene, but without specific characteristics, such as positive anti-human T-lymphotropic virus type I (HTLV-I) antibody and/or monoclonal integration of HTLV-1 proviral DNA in the tumor cells, and appearance of clusters of "clear cells," were classified as PTCL-NOS. Cases showing diffuse proliferation of large B-lymphoid cells with a prominent polymorphous cellular background containing small lymphoid cells, plasma cells, histiocytes, and/or eosinophils that appeared neoplastic were classified as DLBCL-NOS, and cases in individuals >50 years, with the EBV genome in the nuclei of proliferating cells, with no known immunodeficiency or prior lymphoma, were classified as EBV^+ DLBCL-E. LPD that arose in patients treated with immunosuppressive drugs for autoimmune diseases or conditions other than an allograft/autograft transplant setting were classified as other iatrogenic immunodeficiency-associated LPD.

In situ hybridization

RNA in situ hybridization using an EBV-encoded RNA (EBER)-1 probe was performed as described previously [5], with some modifications. Briefly, a 30-base oligonucleotide probe, 5′-AGACACCGTCCTCACCACCCGGGACTTGTA-3′, corresponding to the sense and antisense sequences of a portion of the EBER-1 gene, a region of the EBV genome that is actively transcribed in latently infected cells, was synthesized. The Raji cell line was used as a positive control. As negative controls, hybridizing mixtures containing sense or antisense probes after RNase treatment were used.

Results

Clinical findings

Clinical findings from 19 patients with polymorphous LPD are summarized in Table 1. Patient ages ranged from 28 to 80 (median, 65) years, with a male:female ratio of 7:12. All but one case presented with nodal disease. One case presented with a skin lesion. Three cases had stage I disease, three stage II, five stage III, seven stage IV, and one unknown. No case had a leukemic blood picture or a bulky mass at presentation or during the course. Six cases had histories of RA; five of them received immunosuppressive agents, such as methotrexate, predonisolone, or anti-tumor necrosis factor (TNF)α agents. No patient had a history of AIDS or organ transplantation. Hepatomegaly and/or splenomegaly were found in about half the patients. B symptoms were found in 42% of patients. Serum levels of lactate dehydrogenase were high in 14 of 18 (78%) cases. All patients showed elevated levels of serum soluble IL-2 receptor (the highest value was 29,300 U/mL).

Clonality analysis

DNA was extracted from paraffin-embedded samples and used for PCR-based clonality analysis; DNA was fragmented and unsuitable for analysis in six cases. As a result, clonality analysis on the paraffin-embedded samples was performed in 11 cases (cases 3, 6, 8, 9, 13, 14, 15, 16, 17, 18, and 19; Table 2). Frozen samples were available and used for Southern blot analysis for IgH and TCRβ chain gene rearrangement in 11 cases. In total, clonality analysis was possible in 15 cases: monoclonal proliferation of B and T cells was found in eight and six cases, respectively (Fig. 1a, b); one case (case 14) showed polyclonal proliferation of both the IgH and TCRβ genes. t(14;18)(q32;q21) with the *BCL2-IGH* rearrangement was detected in one case (case 16; Fig. 1c); no case showed t(11;14)(q13;q32) with the *BCL1-IGH* rearrangement. Identical results for clonality were observed in all but one case (case 8), in which Southern blot analysis showed a germline configuration, but the PCR-based method confirmed the presence of a T cell clone.

Pathological findings

Common histological findings in these 19 cases were diffuse, polymorphous cellular proliferation, principally occupying the interfollicular areas, with preservation of lymph follicles in a few cases. Varying numbers of large lymphoid cells were scattered in the polymorphous areas, but their nuclei were neither hyperchromatic nor multilobed, unlike the pleomorphic appearances typically found in the neoplastic proliferation of B and T cells. Mitotic figures were seen occasionally. Vascular proliferation was not marked in any case (Fig. 2).

The WHO classification (2008) was applied to 15 cases for which clonality data were available (Table 2). In the eight cases with monoclonal proliferation of B cells, a mild degree of fibrosis was found in two cases and necrosis in one. Plasma cells were few in number and eosinophils were rarely found. Macrophages were frequently found in three cases, with formation of epithelioid cell clusters in one. Immunohistochemistry revealed diffuse proliferation of

Table 1 Clinical features of 19 patients with polymorphous lymphoproliferative disorder

No	Age	Sex	Immune abnormalities	Immunosupressive agents	Hepatosplenomegaly	BM involvement	B symptoms	IPI	LDH	PS	Stage	Extranodal disease	sIL2R (U/ml)	Follow-up (months)
1	66	F	No	No	No	No	No	L	na	0	1	0	na	60 A
2	59	F	No	No	Yes	No	Yes	na	High	0	3	na	na	32 DT
3	53	F	No	No	Yes	No	Yes	LI	High	0	4	1	3,550	7 DT
4	41	F	No	No	na	Yes	No	HI	WNL	2	4	2	1,750	60 A(PR)
5	80	F	No	No	No	No	No	na	WNL	na	na	na	1,010	46 DID
6	75	F	RA	MTX	Yes	No	Yes	H	High	4	4	1	5,150	11 A(PR)
7	28	M	No	No	Yes	Yes	No	HI	High	1	4	5	1,690	25 A
8	72	F	RA	No	No	No	No	HI	High	0	1	0	2,510	15 DT
9	61	M	No	No	No	Yes	No	LI	High	0	4	1	2,140	20 A(CR)
10	78	F	No	No	Yes	No	Yes	H	High	3	3	na	29,300	3 DT
11	68	F	RA	MTX and PSL	Yes	Yes	Yes	H	High	4	4	1	10,200	24 A
12	76	F	RA	PSL	Yes	na	No	HI	WNL	1	4	2	3,690	1 DT
13	70	M	No	No	na	No	Yes	na	High	na	3	na	4440	3 DT
14	72	F	RA	MTX and anti-TNF α	No	na	No	L	High	1	1	1	573	7 A(CR)
15	78	M	No	No	No	No	No	L	WNL	1	2	0	3,460	5 A(CR)
16	60	M	No	No	No	na	No	na	High	1	2	na	914	na
17	74	M	No	No	Yes	No	Yes	HI	High	1	3	na	4,870	10 A
18	76	M	No	No	No	No	Yes	HI	High	2	2	na	785	1 A
19	49	F	RA	MTX	No	No	No	LI	High	0	3	na	460	5 A(PR)

Abbreviations: *BM* bone marrow, *IPI* international prognostic index, *L* low, *LI* low intermediate, *HI* high intermediate, *H* high, *LDH* lactate dehydrogenase, *PS* performance status, *sIL2R* soluble IL-2 receptor, *F* female, *M* male, *RA* rheumatoid arthritis, *MTX* methotrexate, *PSL* predonisolone, *TNF* tumor necrosis factor, *na* data not available, *WNL* within normal limit, *A* alive, *DT* death due to tumor, *DID* death with intercurrent disease, *PR* partial remission, *CR* complete remission

Table 2 Pathological findings and follow-up data of 15 cases undergoing clonality analysis

Clonality analysis			T cell				Therapy	Complication at presentation	Follow-up (months)	Categorization in WHO classification (2008)
No.	Paraffin	Frozen	EBV	CD4		CD8				
3	T	T	+	+	=	+	CHOP, auto-PBSCT		7 DT	PTCL-NOS
6	T	T	+	+	>	−	MTX withdrawal + mPSL	CAEBV	11 A(PR)	PTCL-NOS
7	nd	T	+	+	=	+	CHOP + allo-BMT	HPS, CAEBV	25 A	PTCL-NOS
8	T	Polyclonal	+	+	>	+	THP-COP, other		15 DT	PTCL-NOS
9	T	nd	−	+	=	+	na		20 A(CR)	PTCL-NOS
19	T	T	−	+	>	+	MTX withdrawal		5 A(PR)	PTCL-NOS
5	nd	B	−	−	<	+	THP-COP, other	Chronic HBV hepatitis	46 DID	DLBCL-NOS
13	B	B	−	+	>	+	R-THP-COP	HPS	3 DT	DLBCL-NOS
15	B	nd	−	+	=	+	R-THP-COP	Type 2 DM	5 A(CR)	DLBCL-NOS
16	B with t(14:18)	B	−	+	=	+	na	Chronic HBV hepatitis	na	DLBCL-NOS
18	B	nd	−	+	>	+	R-THP-COP		1 A	DLBCL-NOS
10	nd	B	+	na		na	R+mPSL+CY	HPS	3 DT	EBV^+ DLBCL of the elderly
17	B	B	+	+	=	+	PSL+CyA	Pure red cell aplasia	10 A	EBV^+ DLBCL of the elderly
11	nd	B	+	+	>	+	mPSL, R+ THP+CY		24 A	Other iatrogenic LPD
14	Polyclonal	nd	+	+	=	+	MTX and anti-TNFα withdrawal		7 A(CR)	Other iatrogenic LPD

Abbreviations: *EBV* Epstein–Barr virus, *nd* not done due to no samples available or severe DNA fragmentation, *na* data not available, *CHOP* cyclophosphamide, doxorubicin, vincristine, and prednisolone, *auto-PBSCT* autologous peripheral blood stem cell transplantation, *R* Rituximab, *THP* pirarubicin, *COP* cyclophosphamide, vincristine, and prednisone, *MTX* methotrexate, *allo-BMT* allogeneic bone marrow transplantation, *mPSL* methylprednisolone, *CY* cyclophosphamide, *PSL* predonisolone, *CyA* cyclosporine A, *A* alive, *DT* death due to tumor, *DID* death with intercurrent disease, *PR* partial remission, *CR* complete remission, *HBV* hepatitis B virus, *CAEBV* chronic active EBV infection, *HPS* hemophagocytic syndrome, *PTCL* peripheral T cell lymphoma, *DLBCL* diffuse large B cell lymphoma, *NOS* not otherwise specified, *LPD* lymphoproliferative disorders

$CD20^+$ large lymphoid cells admixed with $CD3^+$ small lymphoid cells (Fig. 3).

In six cases with monoclonal proliferation of T cells, eosinophil infiltration was marked in three. Plasma cells were occasionally seen in all cases. Macrophages were numerous in three cases, with epithelioid cell clusters in one. Immunohistochemically, $CD3^+$ cells were small-to-medium in size, indistinguishable from reactive lymphoid

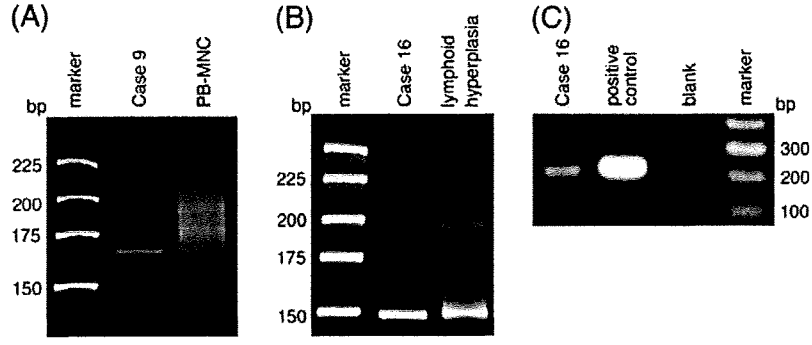

Fig. 1 Clonality analysis using the BIOMED-2 primer set. **a** Case 9 showed T cell monoclonality with the BIOMED-2 TCRG Tube A primer set. **b** Case 16 showed B cell monoclonality with the BIOMED-2 IGK Tube A primer set. **c** t(14;18)(q32;q21) with *BCL2-IGH* rearrangement was also detected in case 16 with the BIOMED-2 t(14;18)(q32;q21) tube A primer set. *PB-MNC* peripheral blood mononuclear cells

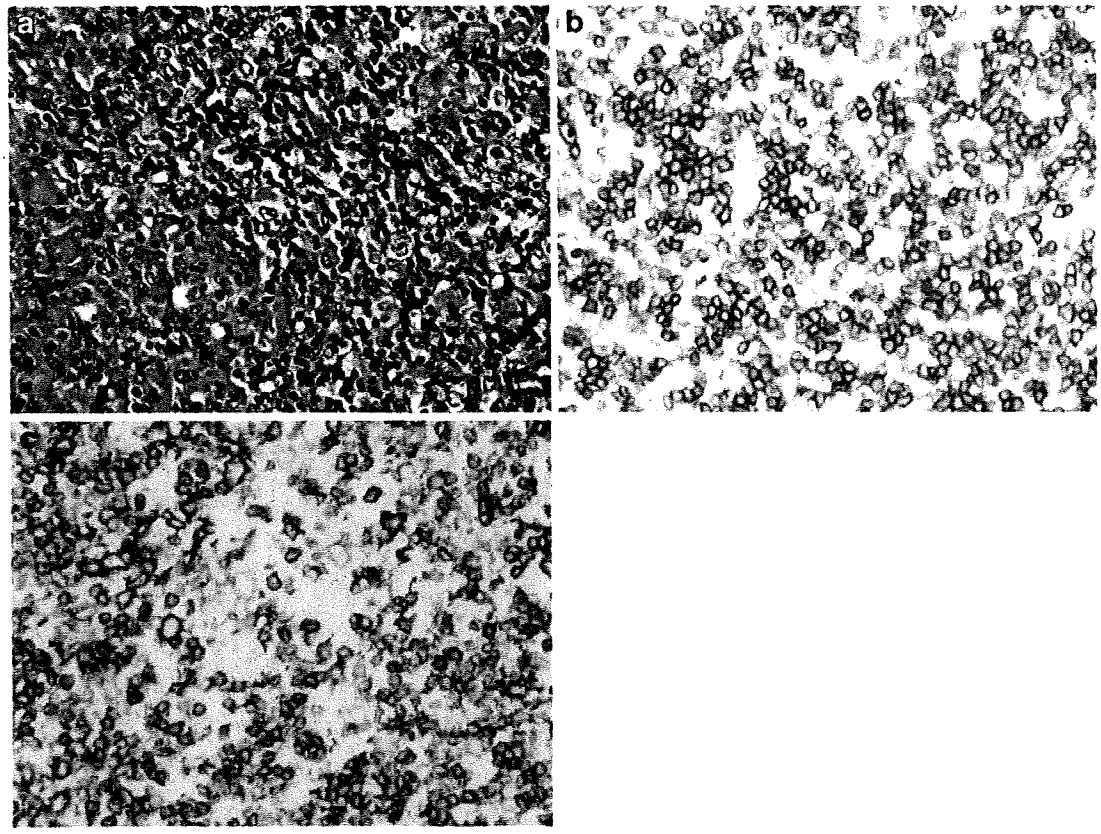

Fig. 2 Diffuse polymorphous proliferation containing large lymphoid cells with prominent nucleoli admixed with small lymphocytes and macrophages in B-LPD (case 18; **a**). An epithelioid cell cluster is seen in the lower left corner. Mitotic figures were seen occasionally (H&E, ×400). Small lymphoid cells were positive for CD3 (**b**), whereas large lymphoid cells were CD20-positive (**c**). This case was classified as diffuse large B cell lymphoma, not otherwise specified, by the WHO classification (2008)

cells. These $CD3^+$ cells were exclusively $CD4^+CD8^-$ in one case, and $CD4^+$ cells predominated or were about equal in number to $CD8^+$ cells in five. $CD20^+$ large lymphoid cells were scattered in four cases.

In one case (case 14) showing polyclonality for B and T cells, large lymphoid cells expressed CD30, but there were no diagnostic RS cells. This case was diagnosed as Hodgkin-like LPD.

Clinicopathological findings in the remaining four cases, in which clonality analysis was not performed, were quite similar to the 15 cases in which it was; thus, it was supposed that these four cases may be neoplastic in nature. Indeed, two of the four patients died due to tumors.

In situ hybridization

RNA in situ hybridization using the EBER-1 probe was performed in all 19 cases. EBV-positive lymphoid cells were detected in eight cases: three of eight cases, four of six cases, and one of one case with monoclonal B, T cell, and polyclonal proliferation. A diagnosis of chronic, active EBV infection was made in two (cases 6 and 7) of these cases at the onset of their LPD. The EBV-positive rate was higher in cases with RA than those without, but not statistically significantly so (p=0.117; Fisher's exact test).

Prognosis

The 3-year overall survival (OS) rate was 49.7±17.3%. Univariate analysis revealed that EBV positivity, history of RA, and B or T cell monoclonality were not prognostic factors. Patients with age ≥70 years showed a worse prognosis than those <70 (33.8±25.1% vs. 57.1±24.9%), but the difference was not statically significant (p=0.091).

Discussion

Through review of clinical and pathological features in more than 4,000 cases of malignant lymphomas and related conditions registered with OLSG, 19 cases (0.43%) were judged to be polymorphous LPD after careful exclusion of reactive changes, PTCL, and HL. Thus, polymorphous LPD is rather rare in Japan. Use of immunosuppressive

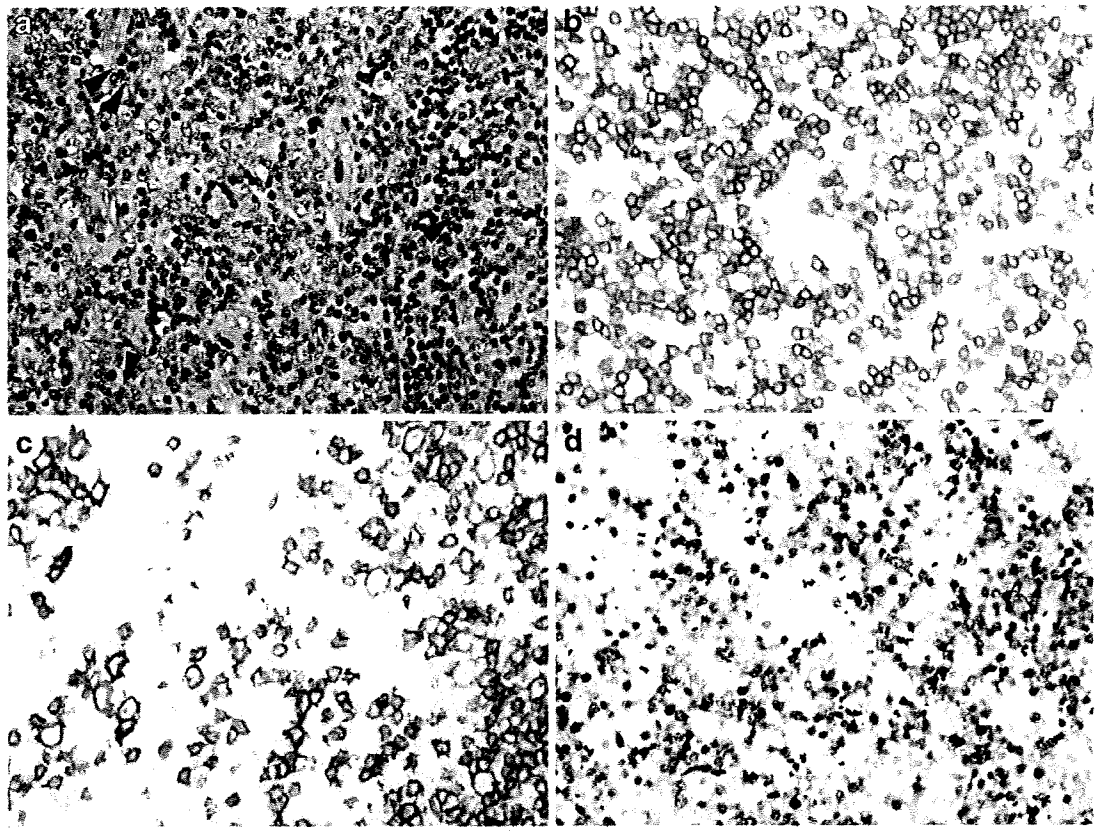

Fig. 3 Diffuse polymorphous cellular proliferation containing medium-to-large lymphoid cells without pleomorphic appearance, small lymphocytes, and eosinophils (*arrowhead*) in T-LPD (case 19; **a**) (H&E, ×400). Small lymphoid cells were CD3-positive (**b**) and medium-to-large lymphoid cells were CD20-positive (**c**). Because PCR clonality analysis by T cell receptor rearrangement revealed T cell clonality, this case was judged to be one of peripheral T cell lymphoma, not otherwise specified, based on the WHO classification (2008). T-LPD and B-LPD could not be distinguished by histological or immunohistochemical features, except for the prominence of eosinophils in the former. In situ hybridization with the EBER-1 probe revealed positive signals in the nucleolus of large lymphoid cells (case 17; **d**)

agents in connection with organ transplantation and AIDS are major causes of polymorphous LPD in Western countries [6–8], but these are less common in Japan [9–11]. This was reflected in the present results: no patient was a transplant recipient or had AIDS.

Molecular analyses revealed that polymorphous LPD was actually a monoclonal proliferation of B (eight cases) or T cells (six cases), intermingled with numerous inflammatory cells. Among 11 cases examined in frozen materials, B or T cell clonality was detected in 10; PCR-based clonality analyses revealed the clonal proliferation of T cells in the remaining case. Except for this case, identical results were obtained between the Southern blot- and PCR-based analyses. Our previous study on MTX-LPD in Japan showed that approximately 80% of cases were B cell in nature [12]. However, the four cases here with MTX-LPD consisted of heterogeneous diseases: T cell LPD with or without EBV, B cell LPD with EBV, and LPD of polyclonal nature with EBV.

The present cases were selected from cases registered with OLSG, based on histological findings of polymorphous composition of proliferation occupying the whole lymph nodal architecture, but devoid of diagnostic RS cells, to exclude HL or medium-to-large T cells with nuclear hyperchromasia and pleomorphic appearances, consisting of multilobed cells, to exclude PTCL-NOS. The proliferating cells were large B-lymphoid cells in the present B cell-proven LPD and medium-to-large T lymphoid cells in T cell-proven LPD. Eosinophils were marked in about half of T-LPD cases, in contrast to the scarcity of eosinophils in the B-LPD cases. One case (case 14) had polyclonal LPD, and the histological picture was HL-like LPD, based on the criteria of Kamel et al. [13].

When the WHO classification (2008) was used, the present 15 cases who underwent clonality analysis were categorized as PTCL-NOS in six cases, DLBCL-NOS in five, EBV^+ DLBCL-E in two, and other iatrogenic LPD in two (Table 2). A possible diagnosis of follicular lymphoma was suggested

in one case of B cell LPD with the BCL2-IGH rearrangement; however, careful observation did not reveal a follicular pattern of proliferation, but showed diffuse proliferation of large B cells, admixed with small T lymphocytes ($CD4^+$= $CD8^+$). This case was tentatively classified as DLBCL-NOS.

Polymorphous LPD is occasionally found in individuals with immunodeficiency conditions. Indeed, six (32%) of the 19 cases had suffered from RA, and two had received MTX (cases 6 and 19), and one each had received MTX and anti-TNFα agents (case 14), MTX and prednisolone (case 11), and prednisolone (case 12; Table 1). Because RA predominantly affects females, inclusion of RA patients resulted in female predominance in the present series.

EBV was detected in eight of 19 (42%) cases: three of four patients with MTX-LPD and five of 15 (33%) non-MTX-LPD cases were EBV-positive. Since Ellman et al.'s first report on lymphoma in a patient with RA who received low-dose MTX [14], a relationship between MTX medication and development of LPD has been discussed [15]. Approximately 50% of MTX-LPD cases are reported to be EBV-positive in the literature [15], and all but one of the present MTX-LPD cases were EBV-positive. MTX may promote the development of EBV-positive lymphomas in RA patients because of its immunosuppressive properties as well as by reactivating latent EBV infection [16]. Previous studies revealed that anti-EBV antibody titers were higher in RA patients, regardless of MTX medication, than in healthy individuals, although proof of a direct causal link between RA and high EBV titer has not been made [17].

The 3-year OS rate in the present series was approximately 50%, which is similar to aggressive non-Hodgkin's lymphoma, where the 5-year OS was reported to be 52% [18]. The four cases with MTX-LPD, including polyclonal LPD (case 14), showed more favorable prognoses. Indeed, when these MTX-LPD cases were excluded, the prognosis in the remaining cases of polymorphous LPD was much worse. Thus, polymorphous LPD should be treated as an aggressive lymphoma. The four cases with no data on clonality of the proliferating cells also tended to show aggressive courses.

In conclusion, the present study showed that polymorphous LPD is (1) quite a rare disease in Japan, (2) MTX-related in some cases, (3) heterogeneous in nature, with mostly monoclonal proliferation of B or T cells, (4) occasionally EBV-associated, and (5) behaves as an aggressive lymphoma. MTX-LPD is a condition closely related to EBV and immunosuppression, and shows a better clinical course than LPD in immunocompetent patients. Polymorphous LPD in the context of immunocompetent patients is biologically and clinically heterogeneous, mostly corresponding to DLBCL or PTCL.

Acknowledgments This study was supported in part by a grant (20014012) from the Ministry of Education, Science, Culture, and Sports, Japan.

Conflict of interest statement We declare that we have no conflict of interest.

References

1. Swerdlow SH, Campo E, Harris NL et al (2008) WHO classification of tumours of haematopoietic and lymphoid tissues. IARC, Lyon
2. Knowles DM (1999) Immunodeficiency-associated lymphoproliferative disorders. Mod Pathol 12:200–217
3. Greer CE, Wheeler CM, Manos MM (1995) PCR amplification from paraffin-embedded tissues: sample preparation and the effects of fixation. In: Dieffenbach CW, Dveksler GS (eds) PCR primer: a laboratory manual. Cold Spring Harbor Laboratory, New York, pp 99–112
4. van Dongen JJ, Langerak AW, Bruggemann M et al (2003) Design and standardization of PCR primers and protocols for detection of clonal immunoglobulin and T-cell receptor gene recombinations in suspect lymphoproliferations: report of the BIOMED-2 Concerted Action BMH4-CT98-3936. Leukemia 17:2257–2317
5. Weiss LM, Jaffe ES, Liu XF et al (1992) Detection and localization of Epstein-Barr viral genomes in angioimmunoblastic lymphadenopathy and angioimmunoblastic lymphadenopathy-like lymphoma. Blood 79:1789–1795
6. Lewin KJ (1997) Post-transplant lymphoproliferative disorders. Pathol Oncol Res 3:177–182
7. Little RF (2003) AIDS-related non-Hodgkin's lymphoma: etiology, epidemiology, and impact of highly active antiretroviral therapy. Leuk Lymphoma 44(Suppl 3):S63–68
8. Martin-Gomez MA, Pena M, Cabello M et al (2006) Posttransplant lymphoproliferative disease: a series of 23 cases. Transplant Proc 38:2448–2450
9 Bando T, Date H, Minami M et al (2008) First registry report: lung transplantation in Japan: The Japanese Society of Lung and Heart-Lung Transplantation. Gen Thorac Cardiovasc Surg 56:17–21
10. Bowman KW, Richard SA (2003) Culture, brain death, and transplantation. Prog Transplant 13:211–215
11. UNAIDS (2007) AIDS epidemic update: December 2007. Joint United Nations Programme on HIV/AIDS (UNAIDS) and the World Health Organization (WHO), Geneva
12. Hoshida Y, Xu JX, Fujita S et al (2007) Lymphoproliferative disorders in rheumatoid arthritis: clinicopathological analysis of 76 cases in relation to methotrexate medication. J Rheumatol 34:322–331
13. Kamel OW, Weiss LM, van de Rijn M et al (1996) Hodgkin's disease and lymphoproliferations resembling Hodgkin's disease in patients receiving long-term low-dose methotrexate therapy. Am J Surg Pathol 20:1279–1287
14. Ellman MH, Hurwitz H, Thomas C et al (1991) Lymphoma developing in a patient with rheumatoid arthritis taking low dose weekly methotrexate. J Rheumatol 18:1741–1743
15. Salloum E, Cooper DL, Howe G et al (1996) Spontaneous regression of lymphoproliferative disorders in patients treated with methotrexate for rheumatoid arthritis and other rheumatic diseases. J Clin Oncol 14:1943–1949
16. Feng WH, Cohen JI, Fischer S et al (2004) Reactivation of latent Epstein-Barr virus by methotrexate: a potential contributor to methotrexate-associated lymphomas. J Natl Cancer Inst 96:1691–1702
17. Toussirot E, Roudier J (2007) Pathophysiological links between rheumatoid arthritis and the Epstein-Barr virus: an update. Joint Bone Spine 74:418–426
18. The International Non-Hodgkin's Lymphoma Prognostic Factors Project (1993) A predictive model for aggressive non-Hodgkin's lymphoma. N Engl J Med 329:987–994

Virchows Arch (2009) 455:285–293
DOI 10.1007/s00428-009-0827-6

ORIGINAL ARTICLE

Diffuse large B-cell lymphoma with a high number of epithelioid histiocytes (lymphoepithelioid B-cell lymphoma): a study of Osaka Lymphoma Study Group

Naoki Wada · Junichiro Ikeda · Masaharu Kohara · Hiroyasu Ogawa · Masayuki Hino · Shirou Fukuhara · Akihisa Kanamaru · Haruo Sugiyama · Yuzuru Kanakura · Eiichi Morii · Katsuyuki Aozasa

Received: 29 April 2009 / Revised: 22 July 2009 / Accepted: 18 August 2009 / Published online: 1 September 2009

Abstract The aim of this study was to clarify whether diffuse large B-cell lymphoma (DLBCL) with a high number of epithelioid histiocytes (DLBCL-EH) could have distinctive clinicopathological characteristics. Clinicopathological findings in 22 cases with DLBCL-EH and, as a control, 96 cases with ordinary type of DLBCL were analyzed. There were ten men and 12 women with ages ranging from 38 to 91 (median, 64) years. The primary site was lymph node in 16 cases, extranodal organs in three, and unknown in three. Stage of disease was I in five cases, II in three, III in nine, and IV in five. Histologically, there was a diffuse proliferation of large lymphoid cells admixed with numerous clusters of epithelioid histiocytes sprinkling throughout the lesions. Immunohistochemically, the large lymphoid cells were $CD20^{+}$, $CD15^{-}$, and $CD3^{-}$ and positive for CD10, bcl-6, and MUM1 in nine (41%), eight (36%), and 12 (55%) of 22 cases, respectively. Epstein–Barr virus positive rate was higher in DLBCL-EH (23.8%) than that in ordinary DLBCL (4.5%; $P<0.05$). Clonality analysis revealed monoclonal bands in all of the examined 20 cases with DLBCL-EH. Multivariate analysis revealed the prominent epithelioid reaction to be an independent factor for favorable prognosis. These findings suggest that DLBCL-EH could be a specific morphological variant of DLBCL associated with a better prognosis.

Keywords B-cell lymphoma · Epithelioid cells · Epstein–Barr virus · Prognosis

Introduction

In the World Health Organization (WHO) classification for lymphoid neoplasias, malignant lymphomas are largely divided into B-cell neoplasia, T/NK-cell neoplasia, and Hodgkin's lymphoma (HL). Diffuse large B-cell lymphoma (DLBCL), the most common category constituting about 30% of all lymphomas in the world, is defined as a diffuse proliferation of large neoplastic lymphoid B cells [1, 2]. Based on this criteria, it is

N. Wada · J. Ikeda · M. Kohara · E. Morii · K. Aozasa (✉)
Department of Pathology,
Graduate School of Medicine,
Osaka University,
2-2 Yamadaoka, Suita,
Osaka 565-0871, Japan
e-mail: aozasa@molpath.med.osaka-u.ac.jp

H. Ogawa
Department of Internal Medicine,
Hyogo College of Medicine,
Nishinomiya, Hyogo, Japan

M. Hino
Department of Clinical Haematology and Diagnostics,
Graduate School of Medicine,
Osaka City University, Osaka, Japan

S. Fukuhara
First Department of Internal Medicine,
Kansai Medical University, Moriguchi, Osaka, Japan

A. Kanamaru
Department of Hematology, School of Medicine,
Kinki University, Sayama, Osaka, Japan

H. Sugiyama
Department of Functional Diagnostic Science,
Graduate School of Medicine, Osaka University,
Suita, Osaka, Japan

Y. Kanakura
Department of Hematology and Oncology,
Graduate School of Medicine, Osaka University,
Suita, Osaka, Japan

postulated that DLBCL comprises morphologically, immunohistochemically, and clinically heterogeneous tumors with each unique clinical and pathologic features. Therefore, attempts have been undertaken to classify the DLBCL into biologically and clinically relevant subgroups. On the basis of the gene expression profile, DLBCL could be categorized into the germinal center B-cell type (GCB) and activated B-cell type (ABC) [3, 4]. Approximately 50% of adult DLBCLs are reported to be GCB subgroup [3].

DLBCL is categorized as one of the aggressive non-Hodgkin's lymphomas (NHL). At present, the International Prognostic Index (IPI) is widely adopted for the prediction of outcome in patients with aggressive NHL [5]. It incorporates patient age, performance status, serum lactate dehydrogenase (LDH), clinical stage, and number of extranodal lesions.

Through a review of cases registered with Osaka Lymphoma Study Group (OLSG), we found 22 cases of DLBCL with a high number of epithelioid histiocytes (DLBCL-EH). Follow-up study revealed that patients with DLBCL-EH showed a much more favorable course than ordinary DLBCL.

Patients and methods

Patients

From November 1999 to December 2007, a total of 3,468 cases were registered with OLSG, Japan. Histologic specimens obtained by biopsy were fixed in 10% formalin and routinely processed for paraffin embedding. Histologic sections, cut at 4 μm, were stained with hematoxylin and eosin and immunoperoxidase procedure (ABC method). All of the histologic sections were reviewed by one of the authors (KA) and classified according to the WHO classification. A diagnosis of malignant lymphoma was confirmed in 2,808 of 3,468 cases (81.0%). Of these 2,808 cases, 2,541 (90.5%) were NHL and 267 (9.5%) HL. The number of DLBCL cases was 1,220, which constituted 48.0% of all NHL. In 22 cases (1.8%) of DLBCL, there was a diffuse proliferation of large B-lymphoid cells admixed with numerous clusters of epithelioid histiocytes sprinkling throughout the lesions mimicking "Lennert lymphoma": They were selected for the present study. Ninety-six cases of DLBCL registered during August 2000–May 2005 were used as the control group (DLBCL-CG) because adequate clinical data and unstained sections for additional immunohistochemical analyses and in situ hybridization were available. Clinicopathological findings of DLBCL-EH and DLBCL-CG are summarized in Table 1.

Adequate clinical information was available in all patients. There were ten men and 12 women with ages ranging from 38 to 91 (median, 64) years. Primary site was lymph node in 16 cases and extranodal organs (spleen, orbit, and spinal epidural region) in three. Primary site could not be defined in three cases due to advanced disease involving both lymph nodes and extranodal organs. On the basis of the records of physical examinations, surgical notes, and pathologic examinations of the specimens, the Ann Arbor staging system was applied. Stage of disease was I in five cases, II in three, III in nine, and IV in five. The IPI score was calculated with five adverse factors (age>60 years, Ann Arbor stages III and IV, Eastern

Table 1 Brief clinicopathological findings

Characteristic	DLBCL-EH	DLBCL-CG	*P* value
Age (years): range (mean/median)	38–91 (65.2/64)[a]	24–86 (62.8/64)[b]	NS
Age>60 years, *n* (%)	17/22 (77.3%)	58/96 (60.4%)	NS
Sex, male/female	10:12	56:40	NS
Primary site, nodal/extranodal	16:3	39:35	0.013
Serum LDH level>normal, *n* (%)	11/22 (50%)	48/96 (50%)	NS
Performance status 2–4, *n* (%)	4/22 (18.2%)	26/96 (27.1%)	NS
Stage 3/4, *n* (%)	14/22 (63.6%)	43/96 (44.8%)	NS
Involved extranodal organ>1, *n* (%)	6/22 (27.3%)	22/96 (22.9%)	NS
IPI, HI/H, *n* (%)	9/22 (40.9%)	39/96 (40.6%)	NS
Response, SD/PD, *n* (%)	3/22 (13.6%)	15/96 (15.6%)	NS
Proliferation pattern			
Monomorphous, *n* (%)	0 (0%)	79 (82.3%)	<0.001
Polymorphous, *n* (%)	22 (100%)	17 (17.7%)	
Fibrosis, present/absent	17:5	47·49	0.016
Mitotic count (/high-power field)			
mean (range)	2.7 (0–8)[a]	3.0 (0–10)[b]	NS
MIB-1,%, mean (range)	57.1 (20–90)[c]	60 (20–90)[d]	NS
GCB/non-GCB	10:12	42:49	NS
EBV positive, *n* (%)	5/21 (23.8%)	2/44 (4.5%)	0.031

DLBCL-EH diffuse large B-cell lymphoma (DLBCL) with a high number of epithelioid histiocytes, *DLBCL-CG* DLBCL-control group, *IPI* International prognostic index, *HI/H* high-intermediate/high, *SD* stable disease, *PD* progressive disease, *GCB* germinal center B-cell type, *NS* not significant

[a] $n=22$

[b] $n=96$

[c] $n=21$

[d] $n=35$

Cooperative Oncology Group performance scores 2–4, elevation of serum LDH, and two or more extranodal lesions) present at the time of diagnosis [5]. For cases under 60 years, an age-adjusted IPI score was applied, in which advanced stage, low performance score, and elevation of LDH were considered as adverse factors [5]. In one patient (67-year-old man) with stage II disease at presentation, lymphadenopathy disappeared without any adjuvant therapy and the complete remission continued for more than 4 years. Chromosomal analysis in this case revealed t(8;14)(q24.1;q32). All of the remaining patients with DLBCL-EH received the combination chemotherapy, cyclophosphamide, doxorubicin, vincristine, and prednisolone (CHOP) in 15 cases, pirarubicin, cyclophosphamide, vincristine, and prednisolone (THP-COP) in three, and etoposide, mitoxantrone, cyclophosphamide, vincristine, prednisolone, and bleomycin (VNCOP-B) in two. One patient underwent combined chemotherapy and radiotherapy. In the latter half of 2003, rituximab was included in the regimen for most patients. Rituximab (R) was used in 14 (63.6%) of 22 DLBCL-EH patients: ten received R-CHOP, two R-THP-COP, one R-VNCOP-B, and one R only. Rituximab was used in 51 (53.1%) of 96 DLBCL-CG patients. There was not a statistically significant difference in frequency of patients receiving rituximab between DLBCL-EH and DLBCL-CG. Clinical outcome was evaluated according to the guidelines of the International Workshop to standardize response criteria for NHL [6]. Recurrence of disease after the chemotherapy was found in three patients with DLBCL-EH: All these patients underwent biopsy.

Immunohistochemistry

Monoclonal antibodies used for immunophenotyping were CD20, CD3, CD8, Bcl-6, MUM1, CD68, MIB-1, CD15, CD30 (Dakocytomation, Glostrup, Denmark, dilution at 1:400, 1:50, 1:100, 1:50, 1:100, 1:100, 1:1, 1:25, 1:50, respectively), CD4 (Novocastra Laboratories, Newcastle, UK, 1:40), CD10, CD23 (Nichirei Biosciences, Tokyo, Japan, used as prediluted antibodies), and programmed cell death 1 (PD-1; abcam, Tokyo, Japan, 1:50). Tonsils with reactive lymphoid hyperplasia served as external control tissues. In MIB-1 staining, the number of positive cells among 300–1,000 large lymphoid cells was counted: MIB-1 index was calculated as positive cells/100 cells.

In situ hybridization

RNA in situ hybridization using the Epstein–Barr encoded RNAs (EBER-1) probe was performed to examine the presence of Epstein–Barr virus (EBV) genome on the formalin-fixed paraffin-embedded sections according to the method previously described with some modifications [7]. Briefly, a 30-base oligonucleotide probe, 5′-AGACACCGTCCTCACCACC CGGGACTTGTA-3′, which was the sense and antisense for a portion of the EBER-1 gene, a region of the EBV genome that is actively transcribed in latently infected cells, was synthesized using a DNA synthesizer. As a positive control, the Raji cell line was used. As negative controls, the hybridizing mixture containing sense or antisense probe after RNase treatment was used. The presence of EBV genomes was evaluated in 21 cases of DLBCL-EH and 44 cases of DLBCL-CG. When the in situ hybridization yielded positive signals in the nuclei of more than 1% of the proliferating cells, such cases were defined as EBV positive.

Clonality analysis with the use of Ig and BCL2-IgH gene rearrangement

One to five sections with 4–10 μm thickness were cut from the paraffin-embedded samples, deparaffinized with xylene, washed with absolute and 70% ethanol, and subsequently digested in lysis buffer (50 mM Tris–HCl, 10 mM EDTA, 150 mM NaCl, 0.5% sodium dodecyl sulfate, and 0.4 mg/l proteinase K) at 55°C for overnight. DNA was extracted with phenol-chloroform extraction-based protocol, followed by ethanol precipitation and re-dissolved in TE buffer. Immunoglobulin (Ig) gene rearrangement was assessed by eight PCRs with 41 primers according to BIOMED-2 protocols [four multiplex PCRs and one single PCR with 28 primers for Ig heavy chain (IgH) gene; two multiplex PCRs with ten primers for Ig kappa light chain (Igκ) gene; one multiplex PCR with three primers for Ig lambda light chain (Igλ) gene] [8]. When the PCR amplification was not sufficient because of small amount of extracted DNA or fragmentation of DNA, we modified PCR condition of BIOMED-2 protocols as described in Table 2. The amplified PCR products were electrophoresed in 5.0% or 6.6% polyacrylamide gel based on fragment

Table 2 Summary of the PCR protocols for the original and modified BIOMED-2 PCR reactions

	Original BIOMED-2	Modified BIOMED-2
PCR reaction mix		
Template DNA	40 ng/50 μL	20 ng/50 μL
dNTP	200 μM	No change
Buffer ($MgCl_2$)	1.5 mM	No change
Primer	0.2 μM	0.5 μM
AmpliTaq Gold	1 U/50 μL	2.5 U/50 μL
PCR run parameters		
Denature	30 s	No change
Annealing	30 s	No change
Extention	30 s	No change
Cycles	35	40

sizes. For detection of BCL2-IgH chimera gene generated by t(14;18)(q32;q21), BIOMED-2 PCR protocol for MBR, 3′MBR, and mcr was applied as described previously [8]. Genotypic study could not be performed in two DLBCL-EH cases because enough amounts of paraffin-embedded materials for DNA extraction were not available.

Follow-up

The DLBCL-EH patients were followed until June 2008; the follow-up periods for survivors ranged from 2.8 to 98.8 (average, 35.1) months. Nineteen of 22 patients were alive at the end of the observation period. The Kaplan–Meier estimated survival rate for the DLBCL-EH at 5 years was 85.9%. As for the control group, the follow-up periods for survivors ranged from 11 to 99 (average, 45) months. Forty-nine of 96 patients were alive at the end of the observation period: 5-year survival rate was 50%.

Statistical analysis

Differences in frequencies of various clinical and pathologic factors between cases with DLBCL-EH and DLBCL-CG were compared with the chi-square test or the Fisher's exact probability test. Differences of means were compared with the *t* test or the Mann–Whitney test. Survival curves and overall survival rates were calculated with the Kaplan–Meyer method and were compared by the log-rank test. Multivariate analysis was performed with the Cox proportional hazard regression model.

Results

Histologic and immunohistochemical findings

Outstanding feature of DLBCL-EH is the presence of numerous clusters of epithelioid histiocytes sprinkled throughout the lesion with appearance of Langhans type or foreign body-type giant cells in two cases; among them, large lymphoid cells were discernible with occasional formation of large areas of the proliferating cells. This histologic appearance could be called lymphoepithelioid lymphoma (Fig. 1). Varying amount of small lymphocytes were present in the lesions but never predominated over the epithelioid histiocytes even when they were numerous. They were predominantly CD8 positive in 13 of 21 cases examined and rather equal in number of CD4- and CD8-positive lymphocytes in the remaining eight cases. Immunohistochemistry of CD4 and CD8 was not available in one DLBCL-EH case. More than 10% of small T lymphocytes were PD-1 positive in three of 21 DLBCL-EH cases. Staining with CD23 revealed the absence of follicular dendritic cells in 18 cases and faintly stained meshwork in two. Plasma cells and eosinophils were frequent in two cases. As a result, all of DLBCL-EH showed a polymorphous pattern of proliferation. Necrotic foci were occasional in three cases. Appearance of fine fibrous tissues in the background of the lesions was more frequent in the DLBCL-EH (17 of 22 cases) compared to that in DLBCL-CG (47 of 96 cases; $P<0.05$; Table 1).

Morphologic appearances of the large lymphoid cells were identical to centroblasts in 13 cases, centroblasts and immunoblasts in five, and unclassifiable because of tissue artifacts in four. Immunohistochemically, the large lymphoid cells were $CD20^+$ (Fig. 1), $CD3^-$, and positive for CD10, bcl-6, and MUM1 in nine (41%), 8 (36%) and 12 (55%) of 22 cases, respectively. DLBCL-EH could be categorized into GCB with $CD10^+$ or $CD10^-$/bcl-6^+/$MUM1^-$ and non-GCB with $CD10^-$/bcl-6^- or $CD10^-$/bcl-6^+/$MUM1^+$ [9]. Ratio of GCB to non-GCB between DLBCL-EH and DLBCL-CG was similar in the present series. Large lymphoid cells were CD15 negative in all cases (0/21) and CD30 positive in three of 20 cases. Mean mitotic count per high-power field and MIB-1 labeling index among large lymphoid cells were 2.7 and 57.1, respectively.

Recurrence of disease was found in three patients: They were biopsied. The histology of two cases was also DLBCL-EH with appearance of Reed–Sternberg (R–S)-like cells and increased number of eosinophils in one. R–S-like cells were never found in the initial biopsy of any cases. In one case, precise evaluation was not possible because of tissue artifacts.

In situ hybridization

In situ hybridization with EBER-1 probe yielded positive signals in the nucleus of large lymphoid cells in five (23.8%) of 21 cases with DLBCL-EH (Fig. 1). Percentage of EBV-positive cells among large lymphoid cells was 3% in one case, 20% in two, 30% in one, and 70% in one. The EBV positive rate in DLBCL-EH was higher than that in two (4.5%) of 44 cases with DLBCL-CG ($P<0.05$). DLBCL-EH in one patient, who showed the spontaneous regression of lymphadenopathy without adjuvant therapy, was EBV positive.

Molecular genetic study

Genotypic study was performed in 20 cases with DLBCL-EH. All cases showed the monoclonal rearrangement of Ig genes with at least one primer. Monoclonal bands for both IgH and Ig light chain (IgL) genes were found in 17 cases, only for IgH gene in one, and only for IgL gene in two (Fig. 2). The BCL2-IgH gene rearrangement was detected in two (10%) of 20 cases examined. Tumor cells in these two cases showed the positive immunoreactivity for CD10.

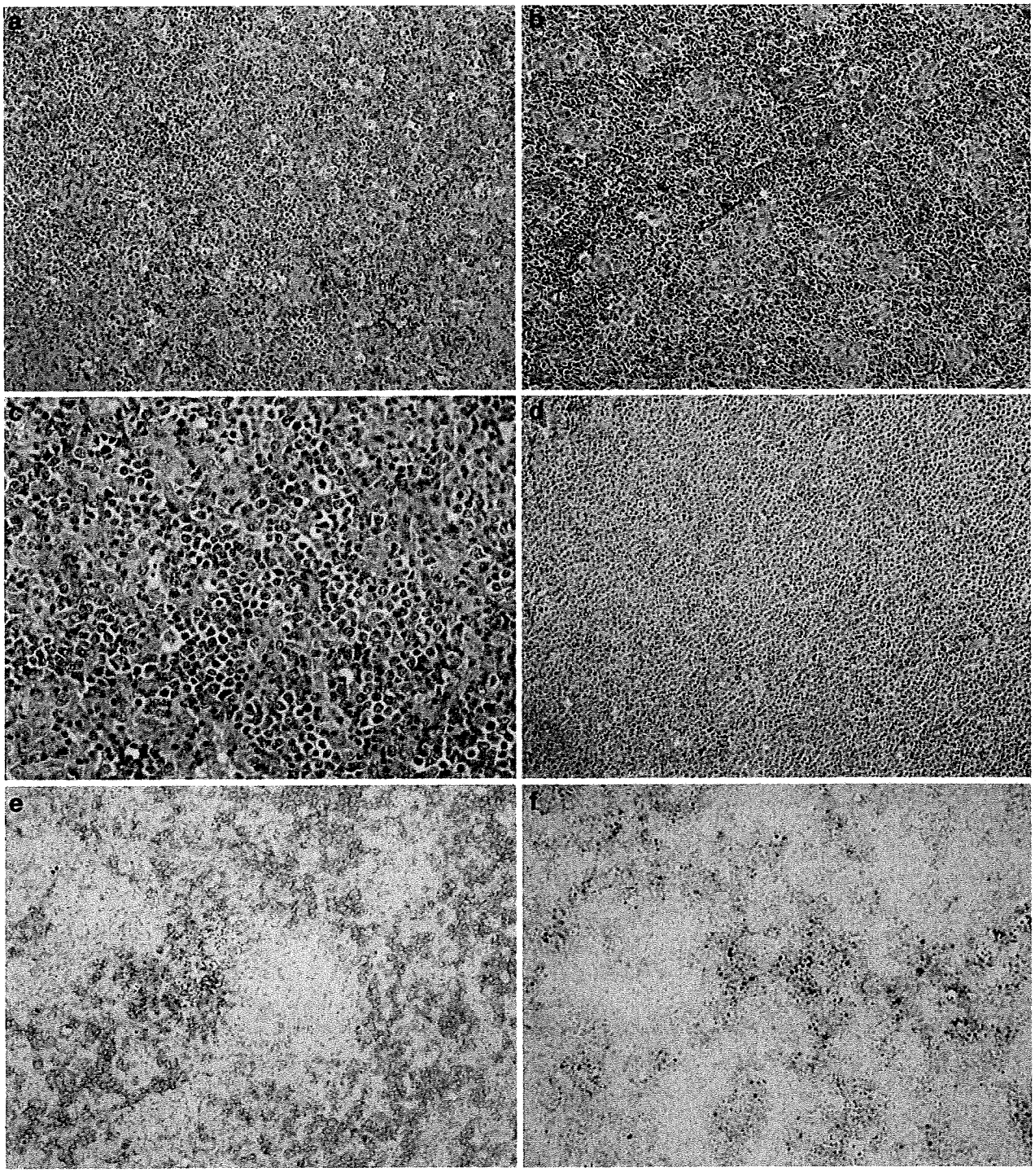

Fig. 1 **a** Diffuse large B-cell lymphoma (DLBCL) with a high number of epithelioid histiocytes (DLBCL-EH). There was a diffuse proliferation of large lymphoid cells admixed with numerous clusters of epithelioid histiocytes sprinkling throughout the lesions. A few small lymphoid cells were found, H&E ×200. **b** Many reactive lymphoid cells were found among clusters of epithelioid histiocytes together with diffuse proliferation of large lymphoid cells in some cases with DLBCL-EH, H&E ×200. **c** Higher magnification illustrating the immunoblast- and centroblast-like proliferating cells in DLBCL-EH, H&E ×400. **d** DLBCL with the ordinary histology showing almost monomorphous proliferation of large lymphoid cells, H&E ×200. **e** Immunohistochemically, the large lymphoid cells in DLBCL-EH were $CD20^{+}$, ×200. **f** In situ hybridization with EBER-1 probe revealed positive signals in the nucleus of large lymphoid cells in DLBCL-EH, x200

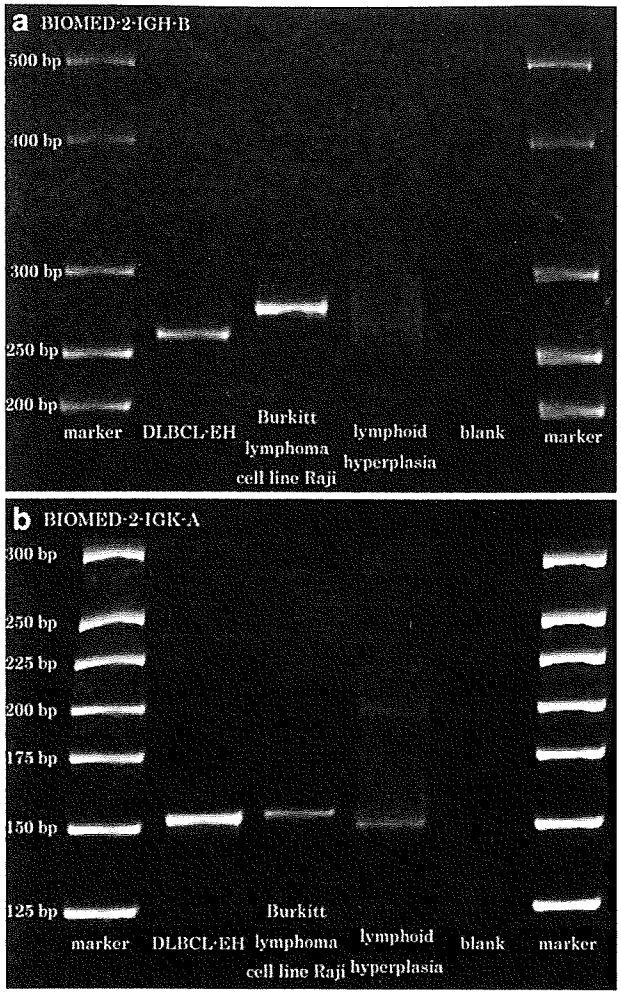

Fig. 2 Clonality analysis with use of immunoglobulin (Ig) heavy chain (IgH) gene (**a**) and Ig kappa light chain (Igκ) gene (**b**). Monoclonal bands were found in lanes of diffuse large B-cell lymphoma with a high number of epithelioid histiocytes (DLBCL-EH) and Burkitt lymphoma cell line Raji

Clinical findings

Brief clinical and pathological findings are summarized in Table 1. There were no findings suggestive of the presence of immunodeficient conditions. Two patients had a past history of autoimmune diseases, one each of idiopathic thrombocytopenic purpura and rheumatoid arthritis. One patient had a past history of chronic hepatitis caused by hepatitis B virus. One patient suffered from chronic hepatitis caused by hepatitis C virus and prostatic cancer. Agents supposed to cause immunosuppression such as methotrexate, steroid, or chemotherapeutic drugs for cancer were never used in these patients. No significant differences were found in age, serum LDH level, performance status, number of involved extranodal organ, IPI, response for chemotherapy, and the ratio of GCB to non-GCB subgroup between cases with DLBCL-EH and DLBCL-CG. Female preponderance and the higher frequency of advanced disease (stage III+IV) were found in DLBCL-EH, but the differences of these factors between DLBCL-EH and DLBCL-CG were not significant. Significant difference was found in the primary site (nodal vs extranodal) between DLBCL-EH (16:3) and DLBCL-CG (39:35; $P<0.05$).

Prognostic factors

The estimated survival rate at 5 years for the DLBCL-EH (85.9%) was significantly higher than that for DLBCL-CG (50%; log-rank, $P<0.05$) (Fig. 3). Results of the univariate analysis are shown in Table 3. Elevated serum LDH level, low PS, advanced stage, involved extranodal organ>1, and high IPI score were unfavorable factors for prognosis. The presence of prominent epithelioid cell response and GCB subgroup were favorable factors for prognosis. Multivariate analysis revealed that low PS was an independent factor for poor prognosis, and prominent epithelioid cell response was a favorable prognostic factor (Table 4). GCB subgroup showed a marginal significance for favorable prognosis ($P=0.062$).

Discussion

In the WHO classification (2008), several variants of DLBCL, not otherwise specified, are listed such as T cell/histiocyte-rich large B-cell lymphoma (THRLBCL), primary DLBCL of the central nervous system, primary cutaneous DLBCL, leg type, and EBV-positive DLBCL of the elderly [1]. At first, a difference of DLBCL-EH from THRLBCL should be commented. The new classification provides a description that "THRLBCL is characterized by a limited number of scattered, large, atypical B-cells embedded in a background of abundant T cells and frequent histiocytes" [10]. In the DLBCL-EH, large B cells are numerous and form sheets of

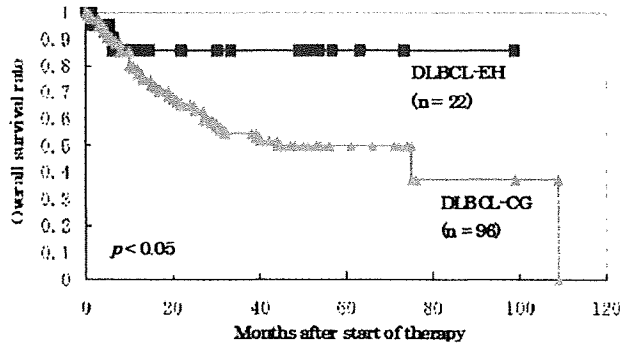

Fig. 3 Overall survival curve for patients with diffuse large B-cell lymphoma (DLBCL) with a high number of epithelioid histiocytes (DLBCL-EH) and DLBCL-control group (DLBCL-CG; Kaplan–Meier method). The estimated survival rate in patients with DLBCL-EH at 5 years (85.9%) was significantly favorable than that in DLBCL-CG (50.0%) (log-rank, $P=0.045$)